

# Typology of seismic motion and seismic engineering design

E. Mistakidis<sup>1</sup>, R. Apostolska (Petruševska)<sup>2</sup>, D. Dubina<sup>3</sup>, W. Graf<sup>4</sup>, G. Necevska-Cvetanovska<sup>2</sup>, P. Nogueiro<sup>5</sup>, S. Pannier<sup>4</sup>, J.-U. Sickert<sup>4</sup>, L. Simões da Silva<sup>5</sup>, A. Stratan<sup>3</sup>, U. Terzic<sup>6</sup>

<sup>1</sup>*Laboratory of Structural Analysis and Design, Dept. of Civil Engineering, University of Thessaly, Greece*

<sup>2</sup>*Institute of Earthquake Engineering and Engineering Seismology, IZIS, University "Ss. Cyril and Methodius", FY Republic of Macedonia*

<sup>3</sup>*Politehnica University of Timisoara, Romania*

<sup>4</sup>*Technische Universität Dresden, Fakultät Bauingenieurwesen, Institut für Statik und Dynamik der Tragwerke, Dresden*

<sup>5</sup>*University of Coimbra and Instituto Politécnico de Bragança, Portugal*

<sup>6</sup>*TEAC, Structural Engineering, San Ramon, CA, USA*

**ABSTRACT:** The paper deals with the influence of the seismic motion typology on the structural response and with engineering design under exceptional actions. Various aspects of seismic motion typology that lead to exceptional actions on the structures are covered. The influence of near fault ground motions, the effect of local site parameters and the magnification of the seismic action on short-period structures are among the parameters identified as dominant for the structural response. The paper presents also a methodology for handling uncertainty in engineering design, based on the mathematical framework of fuzzy analysis. Finally the paper presents various applications of performance based design, which is viewed as a tool for the analysis of structural behaviour under extreme seismic events. The influence of connection behaviour on the structural response is studied, and applications of the capacity design methodology and of the direct displacement design approach for the evaluation of reinforced concrete structures are presented.

## 1 INTRODUCTION

The case of earthquake forces on structures is a rather characteristic case where an action can be exceptional. It is admitted that there exists a high probability that the value of the seismic forces will at some time exceed the value prescribed in the design. This fact is related to the inherent uncertainty nature of the seismic action but also to incomplete or inadequate knowledge of the structural behavior at the time of the design of the structures.

From the viewpoint of the seismology, it is well known that it is difficult to obtain exact values for the seismic actions. For example, during the past 20 years, a significant number of recorded strong motion data has indicated that the characteristics of the ground motion vary significantly between recording stations. This phenomenon is magnified for stations located near the epicenter. As a result, two main regions with different types of ground motions can be considered, the near-source region (i.e. the region within few kilometers of either the surface rupture or the projection on the ground surface of the fault rupture zone) and the far-source region situated at some hundred kilometers from the source.

Unfortunately, the characteristics of the design spectra and the design methods adopted by the majority of the seismic codes have been based on records obtained by far-source fields and, therefore,

they are incapable to describe the seismic intensity in the near-source region. Moreover, the vertical component of the seismic action in near-source field could be greater than the horizontal ones. Also, in near-source areas, due to the very short periods of the ground motion and the pulse characteristics of the loads, the significance of higher vibration modes increases. Due to the pulse characteristics of the actions, developed with great velocity and especially due to the lack of restoring forces, the ductility demands could be very high.

Another aspect of the seismic design whose significance has been recognized only during the last decades is connected to the ground conditions. It is now well known that the properties of the site soils affect the intensity of shaking that can be expected at the building site. Various parameters such as the thickness of the soft and stiff soil layers, the shear wave velocities of the rock and soil layers, the soil/rock impedance ratio, the layering properties of the soil layers etc. influence the amplification or attenuation of the seismic action on the structures.

Another reason leading to exceptional accelerations on structures (i.e. accelerations greater than the design ones) is connected with magnification that sometimes occurs in the short period range.

The present paper, in its first part (sections 2-5) contributes mainly in the above mentioned topics. In Section 2, the emphasis is given to seismic motions with specific characteristics that lead to exceptional actions on structures. Near-fault ground motions and the local site parameters are examined and the latest developments in the field are presented. Section 3 deals with the modeling of the ground motion specifically for the needs of the seismic analysis of structures. Section 4 studies the behaviour of structures in the short period range and the corresponding magnification of the seismic action that has been observed. Section 5 presents in a mathematically abstract way the procedure that can be applied in order to handle uncertainty in structural analysis. Both the cases of uncertainty in the seismic motion parameters and uncertainty in the model parameters are covered.

Except of the cases identified earlier, there are also reasons more closely connected to the structural system, for which a structure might be submitted to an exceptional earthquake action. For example the behaviour of the connections in steel structures has been identified as crucial for the structural response after the Kobe and Northridge earthquakes. Similarly, concrete structures suffer from micro-cracks induced by relatively moderate earthquakes that influence the structural response under design-level earthquakes. Also the case of rather old existing structures has to be identified as one where the seismic events may be exceptional due to the fact that a lot of changes have been introduced during the last years concerning the design seismic forces on structures. The second part of the paper (Section 6) deals with some of the above problems using the performance based design framework as a tool for the analysis of the structural behaviour under extreme (in the previous sense) seismic events. Section 6.2 deals with the influence of connection behaviour on the seismic response of structures. Section 6.3 presents a capacity design methodology for the design and evaluation of the seismic resistance of reinforced concrete structures. Finally, Section 6.4 presents a direct displacement-based design approach for the design of reinforced concrete structures.

## 2 SEISMIC MOTION LEADING TO EXCEPTIONAL ACTIONS ON STRUCTURES

### 2.1 Near-fault ground motions

Characteristics of ground motions recorded in the vicinity of the seismic source can be very different from those recorded away from it.

In the case of near-field ground motions, with the distance to the fault up to 20-60 km, the azimuth of

the site with respect to the hypocenter may affect considerably the characteristics of the seismic motion. The effect of forward directivity is produced when the rupture propagates towards a site and the slip takes place also towards the site (Stewart et al., 2001). Due to the fact that velocity of fault rupture is close to the shear wave velocity, an accumulation of energy is observed at the rupture front. Ground motion in a site affected by forward directivity has the form of a long duration pulse. This effect is characteristic of the fault-normal component of the ground motion. When the rupture propagates away from the site, seismic waves arrive distributed in time. This effect is called backward directivity and is characterised by longer duration and lower amplitudes of the seismic motion. The effect of forward and backward directivity is exemplified for the case of a strike-slip fault in Figure 2.1 (Landers 1992 earthquake).

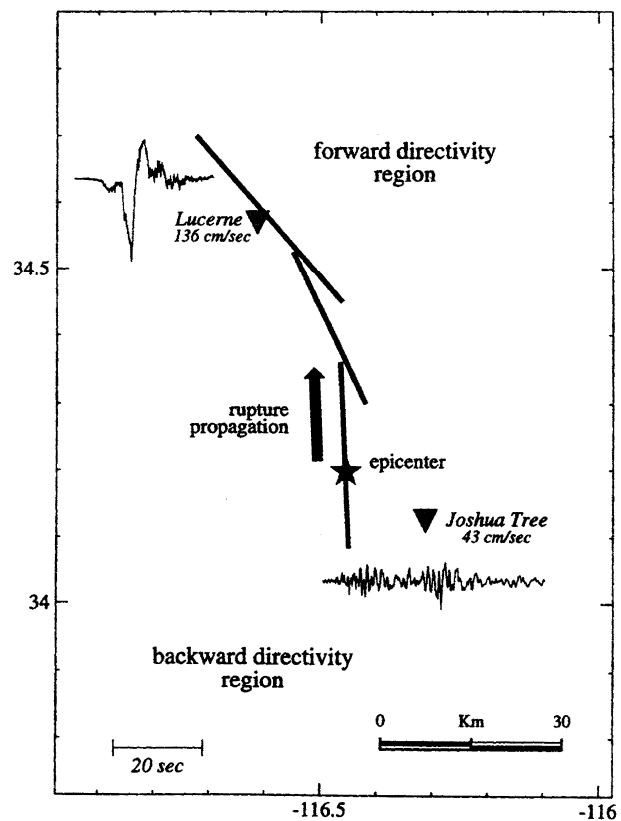


Figure 2.1. Effect of directivity on ground velocity time history, Somerville et al., 1997, in Whittaker, n.d.

Directivity effects can be present both in the case of strike-slip and dip-slip faults (Stewart et al., 2001). In the latter case, forward-directivity effects are observed near the up-dip projection of the fault plane, where characteristic pulse forms in the fault-normal direction.

Despite the fact that ground motion recordings as old as 1950's provided evidence of severe pulse-type characteristics of near-fault ground motions, only recently the importance of near-fault ground motions has been recognized (Sasani and Bertero, 2000). Earthquakes of Northridge (USA, 1994), Kobe (Japan, 1995) and Chi-Chi (Taiwan, 1999) could have

contributed to this by provided a wealth of near-fault strong-motion recordings.

Near-fault effects are still scarcely represented in design codes. Uniform Building Code (1997) provides a near-fault amplification factors to be applied to the design spectrum. However, it does not change the frequency content of the design seismic action. Other seismic design codes, like Eurocode 8 (prEN 1998, 2003) ignore completely near-fault effects.

Vertical component of the ground motion is generally smaller than the horizontal ones, and its effects on structural response is generally ignored. However, in the near-fault regions, vertical component of the ground motion may be important (Gioncu and Mazzolani, 2002) and its influence on seismic performance of structures deserves attention. Vertical component is believed to have contributed to some brittle failure modes in steel structures during the Northridge (1994) and Kobe (1995) earthquakes (Gioncu and Mazzolani, 2002).

## 2.2 Local site conditions

Local site conditions have been recognized for a long time as important parameters affecting ground motion characteristics. Recordings of strong-motion vary significantly with respect to (Stewart et al., 2001):

- local geotechnical conditions,
- possible basin effects, and
- surface topography.

From the above factors, local geotechnical conditions were studied in most detail. Studies performed by Idriss et al. (in NEHRP 2000) show a dependence of the amplification of peak ground acceleration (PGA) by the soil layers on the intensity of the ground motion. Amplification is maximum (between 1.5 and 4.0) for small values of PGA at the base rock (0.05 - 1.0 g), and tends to decrease for ground motions of larger intensities (factors close to 1.0 for values PGA at the base rock about 0.4 g). Reduced amplification of at large intensities is attributed to nonlinear soil response.

Influence of soil types on frequency content of the ground motion is presented in Figure 2.2, according to a statistical study by Seed et al., 1976 (in NEHRP 2000), based on a set of 104 accelerograms recorded in USA, Japan, and Turkey. The effect of soft soil conditions is a significant amplification of spectral accelerations in the medium and long period range (periods larger than 1 second).

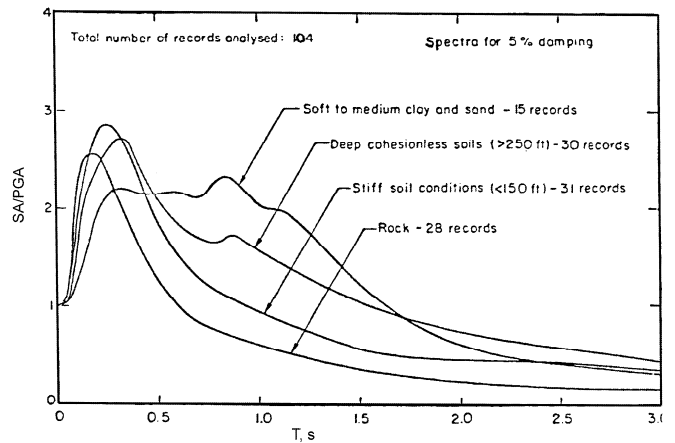


Figure 2.2. Normalised acceleration response spectra for different soil types Seed et al., 1976, in NEHRP 2000.

An example of the effect of soft soil response on the characteristics of the seismic motion is presented in Figure 2.3, for the Vrancea earthquake of 04.03.1977. Horizontal spectral acceleration is greatly amplified in the 1.0-1.5 sec period range, especially for the NS component. The shear wave velocity in the upper 30 m for this site is  $V_{S,30}=130$  m/s (Ambraseys et al., n.d.), while the average shear wave velocity to the bedrock at 128 de m depth is 346.1 m/s (Lungu et al., 1998). The predominant period of vibration of the soil layers inferred from the latter value is  $T_p=1.48$  sec, close to the range of maximum spectral value. Amplification of the ground motion by the soil layers is demonstrated by the high ratio of horizontal to vertical components of response spectra for periods around 1.5 seconds. The ratio of horizontal and vertical spectral ordinates form the basis of the Nakamura method to detect nonlinear soil response (Lacave-Lachet et al., 1998), and is based on the observation that vertical component of the ground motion is affected in a lesser extent by soil characteristics than the horizontal components.

A great deal of site effects may be explained by the dynamic response of the soil layers, assuming horizontal layers and a 1-D wave propagation model. However, there are cases when this assumptions are no longer valid, such as in the case of basins (Graves, 1993, in Stewart et al., 2001). If the seismic wave enters the basin through its edge, it may be "trapped" inside the basin. The effects of multiple reflections are the amplification and increase of duration of the seismic motions. Modelling of these phenomena requires 2-D or 3-D analysis.

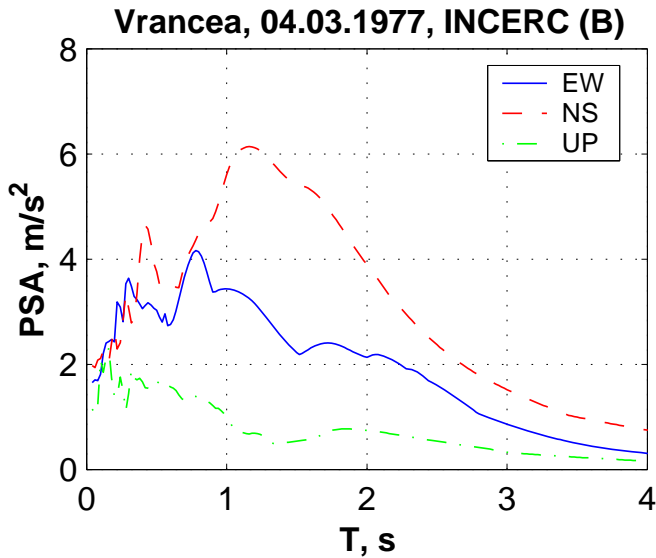


Figure 2.3. Normalised acceleration response spectra for different soil types Seed et al., 1976, in NEHRP 2000.

Amplification of seismic motion may be observed as well for irregular topographies, such as crest, canyon, and slope. A description of a typical topographic amplification was described by Castellani et al. 1982 (in Athanopoulos et al., 1998).

### 2.3 Influence of frequency content of ground motion on inelastic structural response

Most structures are designed to earthquake forces significantly smaller than the ones corresponding to an elastic response. This procedure relies on the observation that structures designed for a fraction of the force corresponding to elastic response are able to survive a major earthquake without collapse (but with important structural damage), due to capacity of the structure to deform in the inelastic range. Earthquake force reduction factors (behaviour factor  $q$  in Eurocode 8, 2003 and  $R$  factor in UBC, 1997) are used in seismic design codes in order to reduce elastic seismic demands to design ones. Code reduction factors are mostly empirical, and are based on observations of past performance of different structural systems (Fischinger and Fajfar, 1994).

Available ductility  $\mu$  of the structural system has a major contribution to the force reduction factor. However, code-specified reduction factors are not based on ductility alone, but also on overstrength. Therefore, code-specified reduction factors can be expressed as:

$$R = R_{\mu} \cdot R_S \quad (2.1)$$

where  $R_{\mu}$  is the ductility-related force reduction factor and  $R_S$  is system overstrength.

Considerable attention was paid in the past on understanding the relationship between the ductility-related force reduction factor  $R_{\mu}$  and ductility  $\mu$ , based on dynamic analysis of single degree of freedom systems. One of the well known studies is that

of Newmark and Hall (1982), who established that  $R=1$  for very short period systems ("equal force rule"),  $R = \sqrt{2\mu - 1}$  for short-period structures ("equal energy rule"), and  $R=\mu$  for medium-and long-period systems ("equal displacement rule").

Later studies recognized the strong dependence of ductility-related force reduction factors on soil type, and, more generally, on the frequency content of the ground motion (Cuesta et al., 2003). Most often, for the scope of deriving relationships between the ductility and ductility-related force reduction factor, frequency content of the ground motion is quantified by the control period  $T_C$ , representing the boundary between constant acceleration and constant velocity regions of response spectra. One of the simple relationships, developed by Vidic et al., 1994 and later modified by Cuesta et al., 2003 was adopted in FEMA 356 and Eurocode 8, in the context of displacement-based analysis procedures:

$$R_{\mu} = \begin{cases} (\mu - 1) \frac{T}{T_C} + 1 & \text{for } T \leq T_C \\ \mu & \text{for } T > T_C \end{cases} \quad (2.2)$$

This relationship is represented schematically in Figure 2.5, and shows that the ductility related force reduction factor ( $R_{\mu}$ ) decreases for systems with period of vibration lower than the control period  $T_C$ . This is equivalent to saying that ground motions with control period  $T_C$  larger than period of vibration of the system impose very larger ductility demands on this system.

Influence of the ratio between period of vibration of the system and the control period  $T_C$  of the ground motion on the  $R_{\mu}$ - $\mu$  relationship is exemplified in Figure 2.4 for the NS component of the INCERC Bucharest record of the 4/03/1977 earthquake. In this figure  $R_{\mu}$ - $\mu$  relationship is shown for several elastic-perfectly plastic (EPP) systems with different periods of vibration. The  $R_{\mu}$ - $\mu$  relationship from Figure 2.4 is a normalized representation of an incremental dynamic analysis (relationship between a measure of ground motion intensity and displacement demand). It can be observed that for systems with the initial period less than  $T_C=1.42$  sec ( $T=0.2$ ,  $0.5$  and  $1.0$  sec), even a small reduction of yield force ( $R_{\mu} > 1$ ) leads to a rapid increase of ductility  $\mu$ . For SDOF periods larger than  $T_C$  ( $T=1.5$  and  $2.0$  sec), ductility demand in the EPP system increases at a lower rate, displacements being even lower than in the elastic system.

Though control period  $T_C$  is a rather simple measure of the ground motion characteristics, it is an important parameter that reflects high ductility demands that can be imposed on structures with fundamental period of vibration lower than ground motion control period  $T_C$ . Ground motions with high frequency content at relatively long periods ( $T_C > 1$

sec) may be generated by (1) very soft soils and (2) forward directivity effect in the case of near-field ground earthquakes.

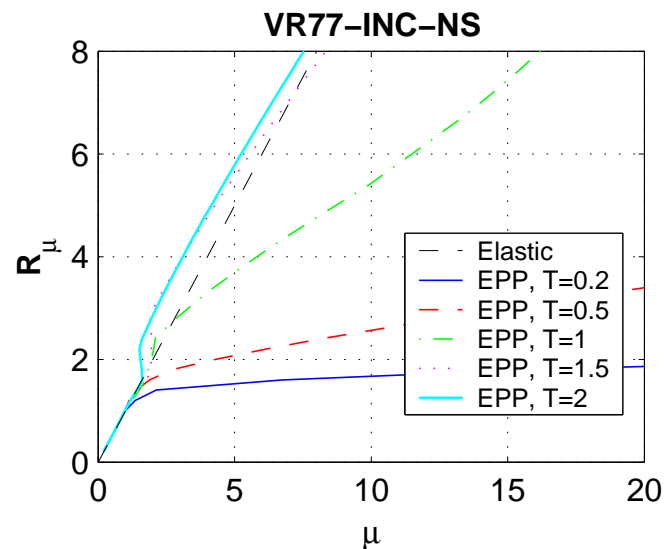


Figure 2.4. Incremental dynamic analysis for EPP systems with period of vibration between 0.2 and 2.0 sec, VR77-INC-NS record.

To check these affirmations, a number of 496 components of earthquakes of magnitude between 6.5 and 7.8 from the European strong-motion database (Ambraseys, n.d.) were analysed (Stratan, 2003). Only the records having effective peak ground accelerations larger than  $0.9 \text{ m/s}^2$  were retained. The obtained ground motions were further grouped in two sets, function of their control period  $T_C$ : group 1, with  $0.3 \leq T_C \leq 0.4 \text{ s}$ , and group 2, with  $1.1 \leq T_C \leq 1.7 \text{ s}$ . Group 1 consisted in 11 records, all motions being recorded on firm soil sites. Ground motions from the second group (10 records) were either recorded on soft sites or were located close to the fault (distance to fault less than 35 km).

In spite of the strong relationship between the value of ductility related force reduction factor and frequency content of the ground motion (quantified by the control period  $T_C$ ), code specified force reduction factors  $R$  are independent of period of vibration of the system and ground motion characteristics. This simplification is justified by the fact that over-strength of low-period structures is generally larger than the one of medium- and long-period structures (Fischinger and Fajfar, 1994), so that the total force reduction factor  $R$  can be considered approximately constant over the period range of most structural systems (see Figure 2.5).

However, this conclusion may not be adequate for ground motions characterized by very large values of control period  $T_C$ . The largest value of control period  $T_C$  currently codified in Eurocode 8 (prEN 1998, 2003) is  $T_C=0.8$  seconds (for type 1 response spectrum, ground type D), which is well below the values of  $T_C$  that can be generated in case of near-

fault motions or very soft soil conditions. Therefore, it may be appropriate to use smaller force reduction factors for design of structures with fundamental period of vibration smaller than the control period  $T_C$  of the design earthquake.

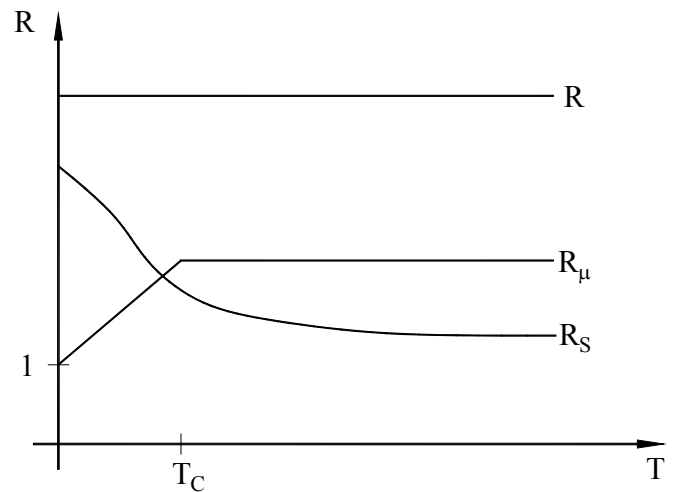


Figure 2.5. Typical qualitative relationship between force reduction factors  $R_\mu$  and  $R_S$ , and period  $T$  (Fischinger and Fajfar, 1994).

A limited study on the performance of moment resisting, eccentrically braced and dual frames designed to Eurocode 8 under ground motions with different frequency content has been performed (Stratan, 2003). Two sets of recorded and semi-artificial accelerograms (seven records in each set) were used, with control periods of  $T_C=0.5$  and  $T_C=1.4$  seconds. Fundamental period of vibration of analysed structures ranged between 0.58 and 0.98 seconds. Significantly larger deformation demands were recorded in the case of  $T_C=1.4$  group of accelerograms, though performance was adequate in most cases. However, other studies (Dubina and Dinu, 2007) indicated that performance of dual concentrically braced frames designed to Eurocode 8 and subjected to the NS component of the INCERC Bucharest record of the 4/03/1977 earthquake was inadequate at the ultimate limit state. A complete study on structures of different system and height is necessary in order to assess if code reduction factors are appropriate for ground motions with large values of control period  $T_C$ .

#### 2.4 Remarks

Directivity effects in near-fault regions and soft soil conditions are two aspects that can generate ground motions with long period pulse-type form. The acceleration response spectrum of this type of motions is characterized by a large value of the control period  $T_C$  (limiting value between the constant acceleration and constant velocity region of the spectrum). While modern design codes generally recognize this effect in the case of soft soil conditions, it is not considered in the case of near-fault ground motions. Structures with fundamental period of vibration

smaller than the  $T_C$  control period of the seismic motion are subjected to increased

A further issue that requires attention and further research is influence of near-fault and soft-soil ground motions on seismic performance of structures with fundamental period of vibration lower than the  $T_C$  control period of the ground motion. Earthquake force reduction factors valid for standard ground motions may be inappropriate in these cases.

### 3 MODELING OF GROUND-MOTION AND SEISMIC ANALYSIS OF STRUCTURES

Traditionally seismic design of structures is based on an elastic structural analysis under reduced seismic forces, accounting for the capacity of the structure to respond in the inelastic range. However, nonlinear analysis methods (time-history and pushover analysis) are increasingly considered in design and especially in research in order to estimate seismic performance of structures.

#### 3.1 Time history representation of ground motion

An important problem when performing a nonlinear time-history analysis is selection of acceleration time histories. Design codes provide a limited amount of guidance on this subject.

Several alternatives can be used when selecting acceleration time histories. Usually the preferred one is to use recorded accelerograms. Design codes require that these records are "adequately qualified with regard to the seismogenetic features of the sources and to the soil conditions appropriate to the site" (prEN 1998, 2003). The straightforward solution is to use recordings at the site of interest obtained in past earthquakes. It is often difficult to find enough strong-motion records in available databases that would match design needs.

Closely related to recorded accelerograms are simulated accelerograms, generated through physical simulation of seismic source, travel path, and local site conditions. Specialized knowledge is required for generating simulated accelerograms.

A further possibility is to use artificial accelerograms, generated so as to match the code elastic spectrum. Eurocode 8 provides a few requirements with respect to the duration of the generated time history and the compatibility between the response spectrum of the generated accelerogram and the target code spectrum. Generally, artificial accelerograms are generated using an inverse Fourier transform of amplitude and phase Fourier spectra.

Figure 3.1 shows an ensemble of five artificial accelerograms generated for different site-source distances, from near field (W1) to far field (W5), Chang and Kawakami, 2006. The same Fourier am-

plitude spectrum, but different phase spectra were used.

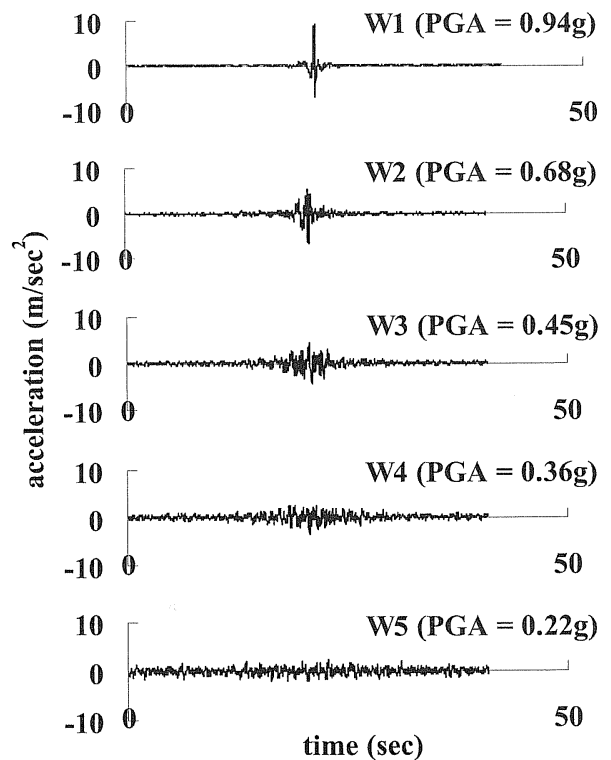


Figure 3.1. Artificial accelerograms, generated for different site-source distances, from near field (W1) to far field (W5), Chang and Kawakami, 2006.

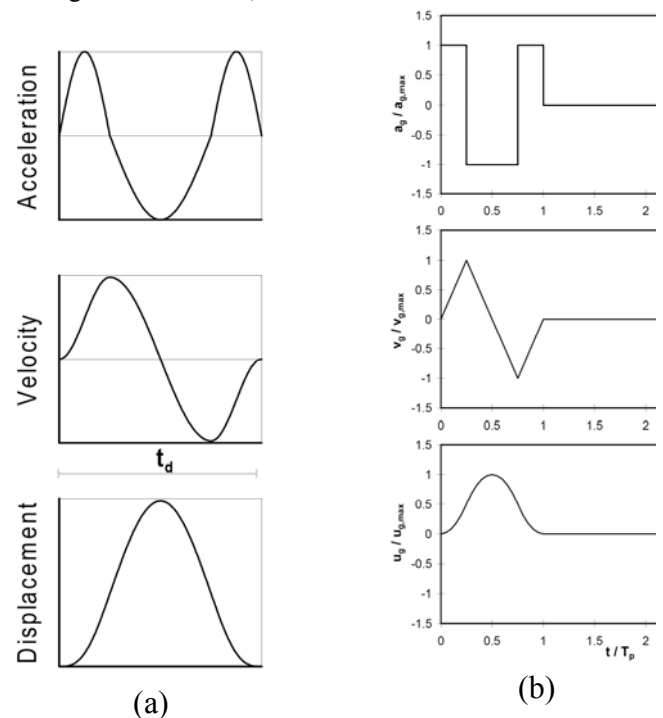


Figure 3.2. Pulse types used to represent fault-normal components of near-fault ground motion by Sasani and Bertero, 2000 (a) and Alavi and Krawinkler (b).

Finally, simple pulses can be used in order to model the ground motion. A review of existing research in this field is available in Gioncu and Mazzolani (2002). Synthetic pulses were used often in studies concerning seismic response of structures under near-fault ground motions. Two types of

pulses used to represent fault-normal components of near-fault ground motions are shown in Figure 3.2.

### 3.2 Pushover analysis

Pushover is a nonlinear static analysis under constant gravity and monotonically increasing horizontal loading. It is described in several design codes and guidelines (prEN1998, 2003; FEMA 356, 2000) and provides an insight into the nonlinear structural response under seismic conditions. Several methods exist that estimate the target displacement corresponding to a given intensity of the seismic action. One of them is the N2 method (Fajfar, 2000) that is implemented in Eurocode 8 (prEN1998, 2003).

Pushover analysis is subjected to several limitations, due to the fact that it relies on the assumption that structural response is governed by the fundamental mode shape, and that this shape does not change when the structure yields under increasing lateral loading. Pushover analysis is mainly applicable to estimating seismic demands on low-rise and medium rise structures in which inelastic demands are uniformly distributed along the height of the structure (Chopra, 2004).

In order to compensate for limitations of the single and invariant lateral load distribution, seismic demands can be obtained on the envelope of demands obtained under several lateral force distributions. For example, Eurocode 8 (prEN 1998, 2003) requires at least two lateral force distributions ("modal" and uniform).

Several improved procedures based on pushover analysis were proposed by different researchers, in order to account for influence of higher modes of vibration and change in distribution of lateral forces as a result of change in dynamic properties of the structure as a result of yielding. A review of different enhanced pushover procedures developed recently are available in Chopra (2004), and Kalkan and Kunnath (2006).

One group of procedures is based on adaptive load patterns, which change at each step of pushover analysis in order to reflect changing in dynamic properties of the structure as a result of yielding. A second group of enhanced procedures is based on modal combination of several pushover analyses with invariant lateral force distributions. While these enhanced procedures eliminate drawbacks of standard pushover procedure, and represent significant advancements of the pushover analysis, their complexity makes it difficult to be implemented in practice.

### 3.3 Conceptual design associated with seismic motion typology

One of the crucial decisions influencing the building structure to withstand earthquakes is the basic plane

shape and configuration. In some extent seismic design codes contain provisions related to building regularity, both in plane and in elevation, and configuration principles related to structural typologies. However, there are two general requests which must be achieved in order to resist severe earthquakes (Bertero, 1997):

- Building structure should be provided with *balanced stiffness and strength* between its members, connections and supports;
- Overall conception and detailing should provide the structure with *balanced overstrength and ductility* of its members and connections in order to possess an enhanced redundancy characterized by the largest number of *defense lines* against seismic action.

Different structures may respond differently to different type of ground motion. Some structural typologies are more sensitive to particular type of motion (pulse, repeated pulses, long duration). In the light of the two previous basic principles, and in order to optimize structural response, the conceptual design of a given structure must always take into account for the specific feature of the possible ground motion.

## 4 MAGNIFICATION OF SEISMIC ACTION ON SHORT PERIOD STRUCTURES

This objective of this section is to study the seismic behaviour of structures in the short period range. The study is performed using a nonlinear SDOF oscillator subjected to various ground motions recorded in Greece. In order to cover various structural typologies, different force-displacement models are used. The study compares the results of the various nonlinear analyses performed with the formulas given in FEMA356 for the estimation of the target displacement using the Displacement Coefficient Method (DCM).

### 4.1 Strong motion data

For the purposes of this study various strong motion data recorded at Greek sites were used. The records used here were selected from a database of about 220 earthquakes recorded in Greece in the period between 1980 and 1999 having a magnitude  $M_L > 4.4$  in the Richter scale and a  $PGA > 0.1g$ .

The records are summarized in Table 4.1.

The characteristic period  $T_g$  of each ground motion was estimated according to engineering judgment to correspond approximately to the period at which the

transition occurs between the constant acceleration and the constant velocity spectrum and at the same time as the lowest period at which the equal-displacement rule holds.

Nu	Code	Station	$M_L$	PGA (g)	$T_g$ (sec)
1	ARGO183-1	Argostoli	6.5	0.171	0.35
2	ATHENS-2	Chanandri	5.9	0.159	0.33
3	ATHENS-3	KEDE	5.9	0.302	0.5
4	ATHENS-4	GYS	5.9	0.121	0.45
5	ARGO183-7	Argostoli	5.7	0.192	0.55
6	ZAK188-4	Zante	5.5	0.170	0.375
7	KAL186-1	Kalamata	5.5	0.273	0.3
8	EDE190-1	Edessa	5.4	0.101	0.4
9	ARGO183-8	Argostoli	5.1	0.305	0.4
10	PAT393-2	Patras	5.1	0.401	0.35
11	LEF194-1	Lefkas	5.1	0.136	0.4
12	KYP187-1	Kyparissia	5.0	0.127	0.25
13	ARGO192-1	Argostolo	5.0	0.204	0.35
14	PYR193-8	Pyrgos	5.0	0.165	0.5
15	KAL286-2	Kalamata	4.8	0.263	0.5
16	LEF188-2	Lefkas	4.5	0.245	0.3
17	IER183-3	Ierissos	4.4	0.178	0.5

Table 4.1 Summary of the motion used in the analysis

#### 4.2 Force-displacement models

The choice of a force-displacement model influences the response time-history and the associated peak response quantities. In order to cover a range of typical structures the following three models were selected, which correspond to different structural characteristics (see Fig. 4.1):

- Type A: an elastoplastic model having a positive post-yield to elastic stiffness ratio of 5%. This type of behaviour is an ideal one and is studied here for reference reasons.
- Type B: a stiffness degrading model with positive post-yield stiffness. This type of behaviour represents wall systems dominated by flexural response, something typical for rather new buildings in Greek territory, dimensioned according to the capacity design principles. The post-yield stiffness was selected to be 5% of the elastic stiffness.
- Type C: a stiffness degrading model with negative post-yield stiffness. This behaviour is a mode typical in wall systems that exhibit some degradation in response with increasing displacement. Degradation may be due to relatively brittle response modes. This is a behaviour typical for rather old buildings in the Greek territory made of masonry, where the strength is reduced for increasing displacements.

The negative post-yield stiffness was selected to be 10% of the elastic stiffness.

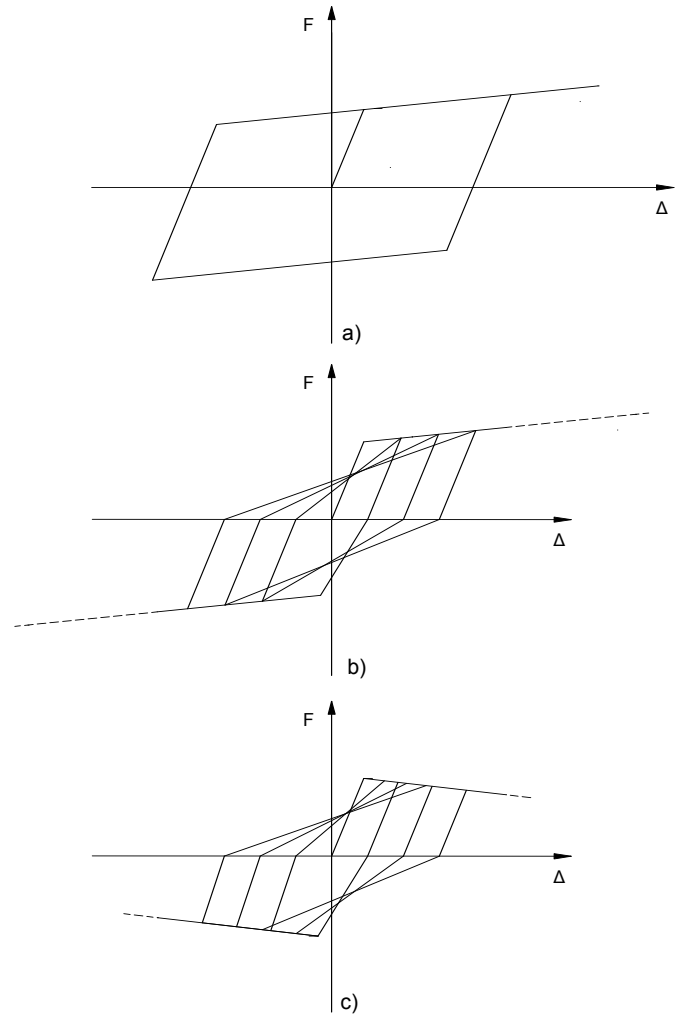


Figure 4.1. The considered force-displacement models

#### 4.3 Dynamic analyses

In the sequel, a time history dynamic analysis was performed on the oscillators corresponding to the models presented earlier. The oscillators were subjected to the 17 ground motions presented in Table 4.1. Two types of analyses were performed.

A. Constant ductility analyses, where the displacement ductility  $\mu$  of the structure was considered as constant and the response of the structure was obtained in terms of different strength reduction factors  $R$ . Five different constant ductility levels were considered corresponding to values of  $\mu$  equal to 1,2,4,6 and 8. For this reason, oscillators were established such as to achieve 20 initial periods of vibration from  $T=0.1$  to  $T=2.0$  sec. At these periods the necessary strength  $F_y$  to obtain design displacement ductilities of 1,2,4,6 and 8 were obtained for each force-displacement model and for each of the ground motions.

Constant strength reduction factor analyses, where the strength reduction factor of the elastoplastic structure was considered as constant and the response of the oscillator was obtained in terms of different levels of the ratio between the peak displacement response of the nonlinear oscillator to the respective one for the linear oscillator. Four different constant strength reduction levels were considered with values of  $R$  equal to 2,3,4 and 5. For this reason, oscillators were established such as to achieve 40 initial frequencies of vibration from  $\nu=0.01$  to  $\nu=10$ . At these frequencies the necessary displacement ductility  $\mu$  to obtain strength reduction factors of 1,2,3,4 and 5 were obtained for each force-displacement model and for each of the ground motions.

It must be pointed out that the actual value of the peak displacement response does not affect directly the results of this study because the oscillator strengths are determined relative to the peak ground acceleration in order to obtain specified displacement ductility demands.

#### 4.4 Results of the dynamic analyses

In the evaluation procedure the attention is given in the estimation of the peak displacement response. It is expected that an acceptable procedure would estimate the peak displacement response of a nonlinear system within acceptable limits of accuracy. For this reason in the figures presented in the following, the ratio  $d_n/d_e$  (referred also in the following as the displacement amplification factor) is studied where:

- $d_n$  is the peak displacement response of the nonlinear oscillator and
- $d_e$  is the peak displacement response of an elastic oscillator having stiffness equal to the initial stiffness of the nonlinear oscillator.

The parameters presented in the figures are:

- The displacement ductility  $\mu$
- The strength reduction factor  $R$  which is defined as the ratio of the elastic strength  $F$  to inelastic strength  $F_y$ .

Figures 4.2 to 4.5 correspond to the first group of conducted analyses, where the displacement ductility was considered as constant. Fig.4.2 depicts the ratio between the peak displacement response of the nonlinear Model-A to the peak displacement response of an elastic oscillator having the same initial period, for  $\mu=4$ . The solid line represents the mean values obtained by the 17 ground motions.

Despite the wide scattering, the mean values seem to follow some rules, i.e. after a characteristic period of about 0.4-0.6 sec, the mean values are close to 1. The divergence from this value increases as the period decreases. Also, the increase of the displacement ductility leads to significant larger mean values in this period range.

Similar are the results for Models B and C but for the sake of brevity are not presented here.

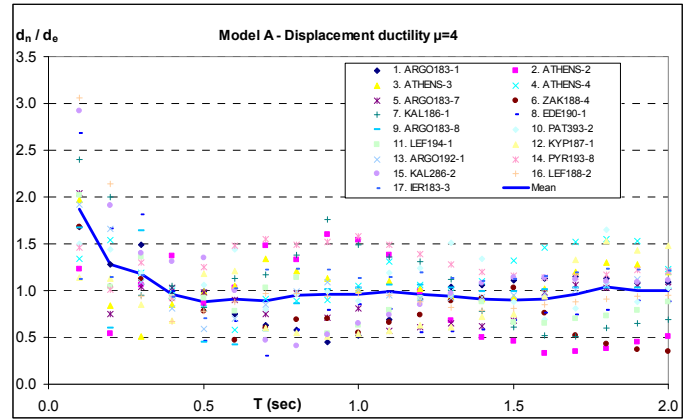


Figure 4.2 Displacement amplification ratio with respect to the period for Model-A ( $\mu = 4$ ).

The analysis results are summarized in the diagrams of Figures 4.3 to 4.5 that depict the mean values and the standard deviation of the results for the three models and for various displacement ductility levels. Notice that although the mean values are close to 1 after a period of 0.4-0.6 sec, the values of the standard deviation differ very much, depending on the displacement ductility level. For  $\mu=2$  the standard deviation takes a rather constant value of 0.2 for all the models considered in this analysis. But, as the displacement ductility increases the values of the standard deviation increase, especially in the short periods range. Also, the standard deviation values seem to be larger in the case of Model-C. Notice also that the mean values for large period systems tend to be somewhat smaller than 1 for Models A and B. That means that the peak displacement response of the nonlinear systems is smaller than the one of the respective linear systems, or equivalently, the response of the linear systems overestimate the response of the nonlinear ones. On the contrary, especially for larger values of the displacement ductility, the results tend to be bigger than 1 for Model-C.

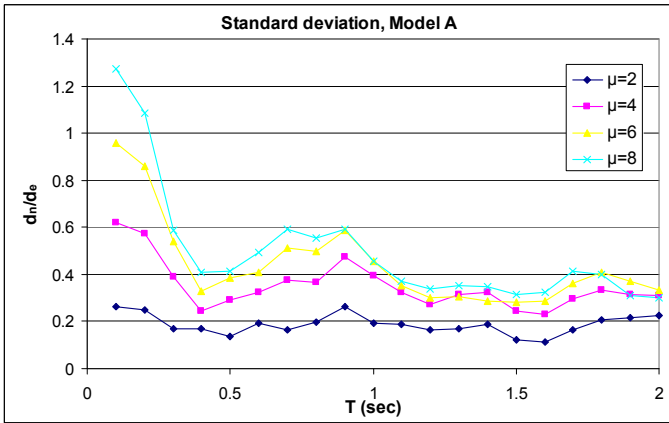
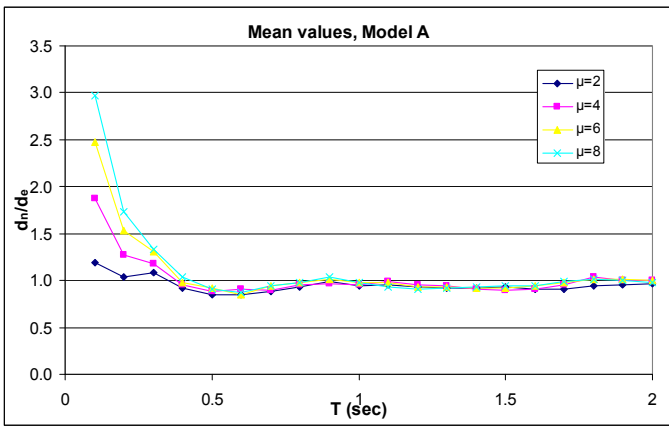


Figure 4.3 Mean values and standard deviation of the displacement amplification factor with respect to the period T for various displacement ductility levels for Model-A.

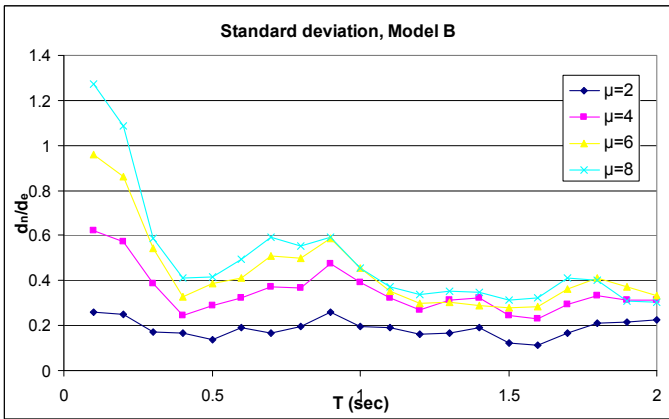
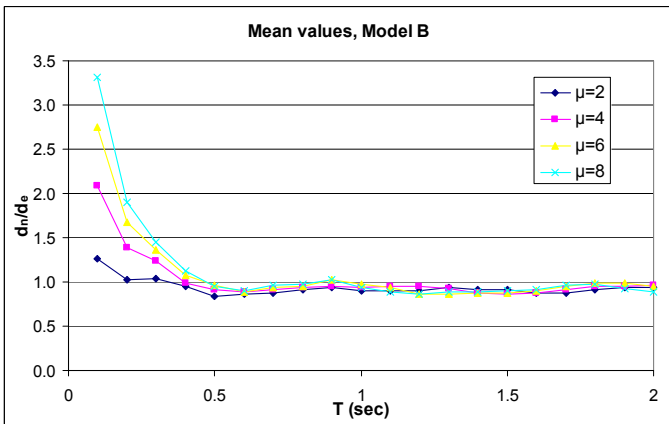


Figure 4.4 Mean values and standard deviation of the displacement amplification factor with respect to the period T for various displacement ductility levels for Model-B.

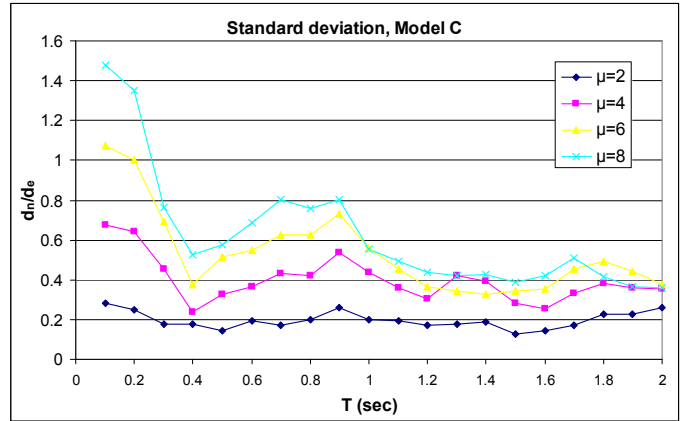
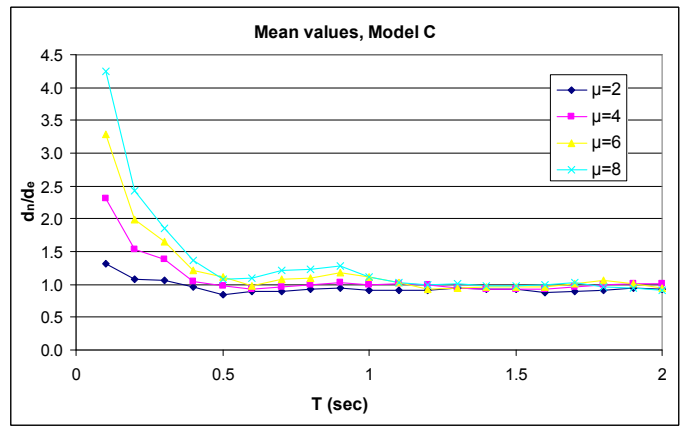


Figure 4.5 Mean values and standard deviation of the displacement amplification factor with respect to the period T for various displacement ductility levels for Model-C.

Figures 4.6 to 4.9 correspond to the second group of conducted analyses, where the strength reduction factor was considered as constant. Fig. 4.6 depicts the ratio between the peak displacement response of the nonlinear Model-A to the peak displacement response of an elastic oscillator having the same initial period, for increasing frequency values, for  $R = 4$ . The obtained values are close to 1 until a characteristic frequency of about 2.5. After this frequency value, the results vary and a great scattering appears. The solid line represents again the mean values of the obtained results. The mean values after the characteristic frequency increase for larger values of  $R$ .

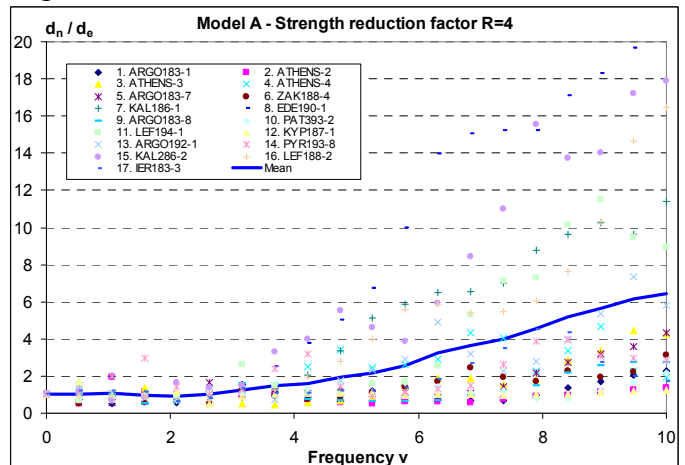


Figure 4.6 Displacement amplification ratio with respect to the frequency for Model-A ( $R = 4$ )

Similar are the results for Model-B, while completely different are the results obtained for Model-C. This model exhibits a negative post-yield stiffness. These models are sensitive to collapse, where collapse is defined as the point at which displacement is large enough that the force resisted by the oscillator tends to zero. Totally, from the 1700 oscillators considered (17 ground motions x 20 frequency values x 5  $R$ -levels) a number of 692 collapsed.

The analysis results are summarized in the diagrams of Figures 4.7 to 4.9 that depict the mean values and the standard deviations of the results for the three models and for various levels of the strength reduction factor. The mean values are close to 1 until a frequency of about 2.5 for all levels of  $R$ . After this frequency, the mean values increase, depending mainly on  $R$ . The values of the standard deviation increase analogously, indicating the great scattering in the ranges of large frequencies. It is again pointed out that the results for Model-C are not representative and are presented only for the sake of completeness.

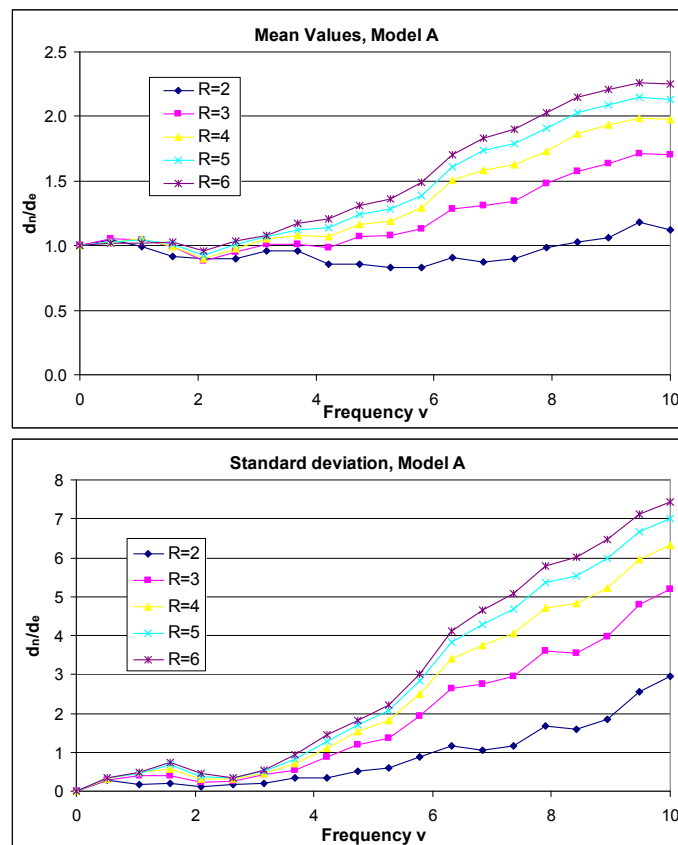


Figure 4.7 Mean values and standard deviation of the displacement amplification factor with respect to the frequency  $v$ , for various values of the strength reduction factor (Model-A)

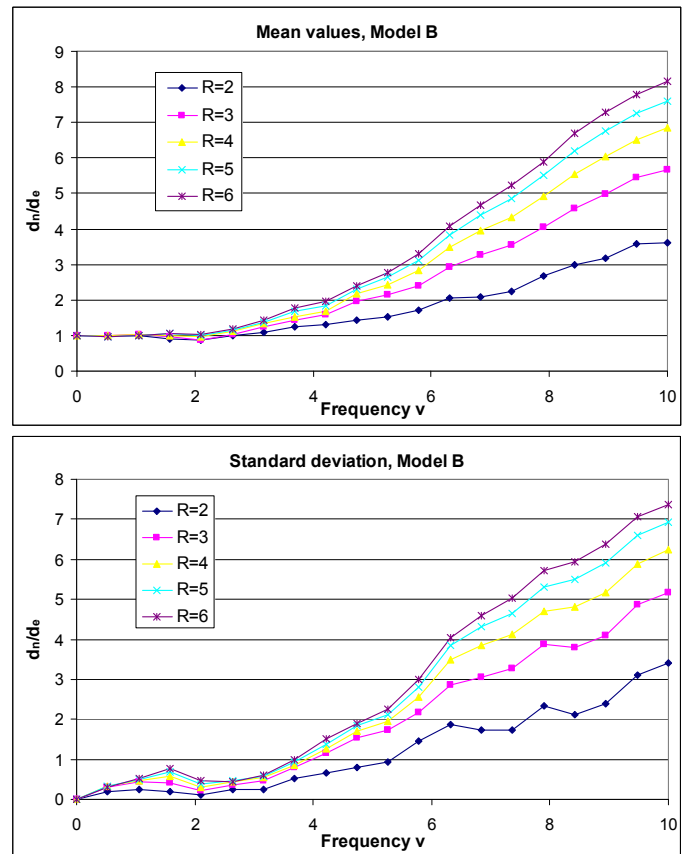


Figure 4.8 Mean values and standard deviation of the displacement amplification factor with respect to the frequency  $v$ , for various values of the strength reduction factor (Model-B)

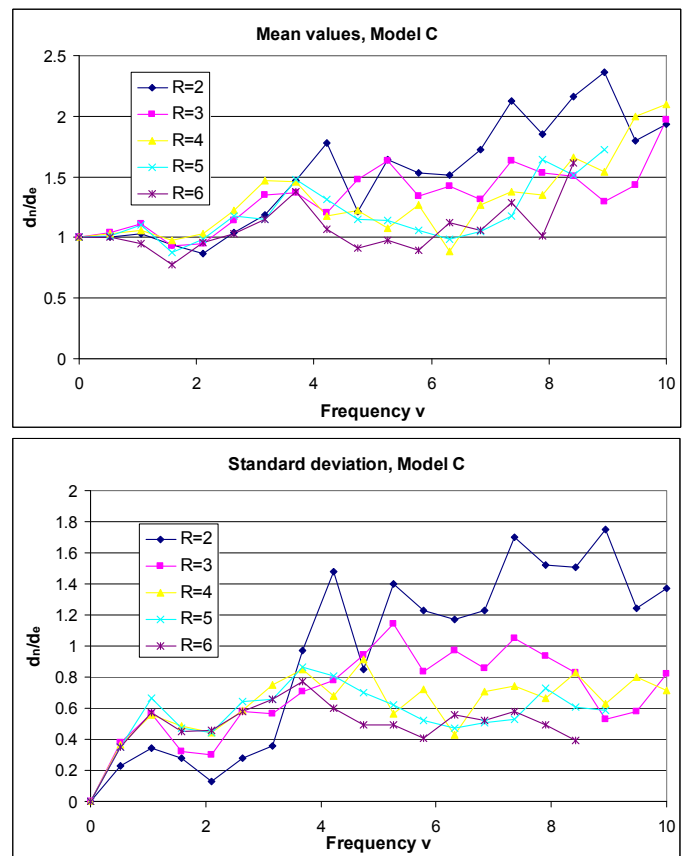


Figure 4.9 Mean values and standard deviation of the displacement amplification factor with respect to the frequency  $v$ , for various values of the strength reduction factor (Model-C)

In Fig. 4.10 the displacement amplification factor is depicted for increasing frequency. Each diagram corresponds to different level of the strength reduction factor and contains the mean values obtained for the three models and also the plot of the results obtained by applying the formulas of the Displacement Coefficient Method (DCM) as presented in FEMA356 for  $T_2 = 0.4$ .

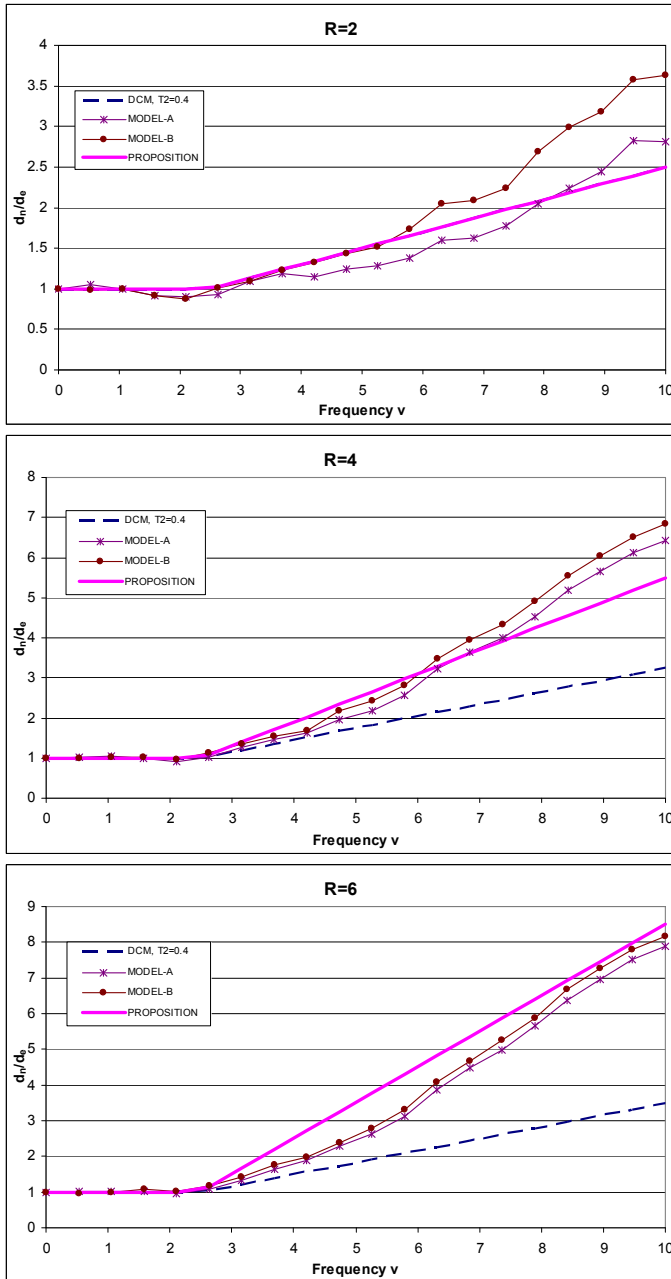


Figure 4.10 Comparison of the results for models A and B with those of DCM

These diagrams actually depict the ability of the coefficient  $C_1$  of DCM to describe the “mean” behaviour of inelastic systems. For low frequencies ( $v < 2.5$ ) it seems that the value of  $C_1$  is reliable. This remarks is also confirmed by the rather low values of standard deviation obtained in this frequency range. For larger frequency values, there is a strong dependence of the response of the nonlinear systems on the strength reduction factor

$R$ . Although the values of  $C_1$  increase with  $R$ , it seems that the mean values increase with a larger rate with  $R$ . Therefore, it seems that  $C_1$  cannot capture the inelastic response of systems with large  $R$  values.

For this reason, a new formula is proposed for the determination of  $C_1$

$$C_1 = 1 + \frac{(R-1)(T_g/T - 1)}{2} \text{ for } 0.1 < T < T_g \quad (4.1)$$

For  $R = 2$  the above formula gives the same results as the one used for the calculation of coefficient  $C_1$  in FEMA356. However, for  $R > 2$  the proposed formula approximates in a better way the results obtained by various analyzed oscillators. It must be noticed however, that the above study focuses only on a small part of the problem because all the seismic records have a characteristic period of 0.3 - 0.55 sec. That means, that from the above study, no conclusions can be drawn for the behaviour of systems excited by ground motions on soft soils.

## 5 UNCERTAINTY IN EARTHQUAKE ASSESSMENT AND SIMULATION

### 5.1 Conceptual treatment of uncertainty in seismic analysis – introduction of the notion of fuzzy quantities and fuzzy analysis

#### 5.1.1 Classification of uncertainty

Numerical simulations of structures under earthquake loads demand reliable input data as well as analysis models close to reality. In general data and models are uncertain which has a significant influence for the results of the analysis. Therefore the uncertainty has to be described with suitable models and considered within the analysis.

Several kinds of uncertainty are distinguishable depending on the reason of origin. If a random result of an experiment under identical boundary conditions may be observed almost indefinitely, the uncertainty can be considered as stochastic. This stochastic uncertainty is described with methods of probability theory. In contrast to this a deficit of information results if the boundary conditions are subjected to (apparently) arbitrary fluctuations, if a system overview is incomplete or if only a small number of observations are available. This uncertainty is referred to as informal uncertainty. If the uncertainty is quantified by linguistic variables, transformed onto a numerical scale, lexical uncertainty is present.

The reason of uncertainty assigns their character-

ristic. Stochastic uncertainty is associated with the uncertainty characteristic *randomness* quantified mathematically with the aid of random variables. Informal and lexical uncertainty is described with the uncertainty characteristic *fuzziness* dealt on the basis of fuzzy set theory. The uncertainty characteristic *fuzzy randomness* occurs in the case of informally or lexically uncertain statistic inference. The uncertainty is then described mathematically on the basis of the theory of fuzzy random variables (Möller & Beer 2004). Randomness, fuzziness and fuzzy randomness may occur as both data uncertainty and model uncertainty. In the case that an uncertain variable depends on time and spatial coordinates random functions, fuzzy functions and fuzzy random functions are introduced.

For conventional investigations of the loading case earthquake only sparsely information about the earthquake loads exists. Specifying the measure intensity as an interval a classification of seismic zones is available. Each zone is characterized by a dedicated effective acceleration. The spectrum form is independent of intensity.

Additional information can be obtained under consideration of all phases of the earthquake process, from the origin and propagation until the transmission from underground to the structure. The regional specific (zones) and the endangering specific, reflecting the frequency response and the amplitude behavior for endangering levels, can be mathematically quantified with fuzzy quantities. Relevant seismic centers in the environment and the distance dependent decrement of the spectral amplitude are uncertain. Geological conditions, (e.g., stratigraphic sequence, intensification and damping effects) and the registration of cyclic characters (e.g., strong earthquake duration) contain further uncertainty. Precisely because these information about the variables summarized above are not available in a sufficient extent, the formulation of fuzzy quantities is reasonable. The consideration of uncertainty in structural analysis improves the results. A gradual evaluation becomes possible.

In the following informal and lexical uncertainty with the uncertainty characteristic fuzziness is considered. The uncertainty is described and quantified on the basis of fuzzy set theory with the aid of assessed intervals. Utilized the latter for seismic structural analysis deficits of information describing input variables as well as human mistakes and mistakes in fabrication, utilization and maintenance of structures may be considered. Subjective effects and assessments of structural parameters described in an applicable mathematical manner influence the results of structural analysis.

The procedures to consider *fuzziness* in structural analysis are subdivided into fuzzification, fuzzy structural analysis and evaluation of fuzzy results. Fuzzification is the quantification of informal and

lexical uncertainty by means of fuzzy quantities. Thereby the fuzziness of the uncertain physical structural parameters is described mathematical.

### 5.1.2 Fuzzy quantities

Fuzzy quantities  $\tilde{x}$  represent the results of fuzzification on the basis of the fuzzy set theory. Thereby the classical set theory which provides binary assessment to crisp conditions is extended to permit gradual assessment of the membership of elements in relation to a set. This is described with the aid of a membership function.

The membership function  $\mu(x)$  is denoted as standardized, if the maximum functional value is equal to one. If  $\mu(x)$  monotonically decreases on each side of the maximum value the fuzzy quantity  $\tilde{x}$  is referred to as convex (Figure 5.1).

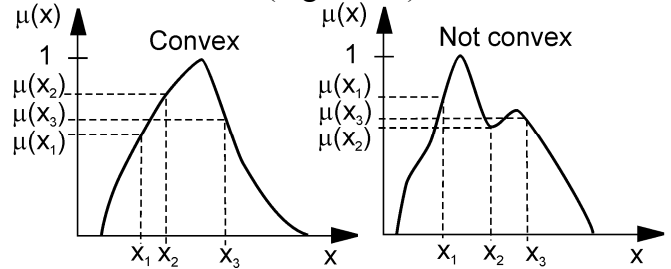


Figure 5.1 Fuzzy quantity  $\tilde{x}$ , convex and not convex

A *fuzzy number* is a convex, standardized fuzzy quantity whose membership function is at least segmentally continuous and has the functional value  $\mu(x) = 1$  at precisely one of the  $x$  values. In extension to this, a *fuzzy interval* has an interval  $[x_1, x_2]$  whereby all elements of  $[x_1, x_2]$  possess the membership  $\mu(x) = 1$ .

From the fuzzy quantity crisp sets  $A_{\alpha_k} = \{x \in \mathbf{X} \mid \mu(x) \geq \alpha_k\}$  may be extracted for real numbers  $\alpha_k \in (0, 1]$ . These crisp sets are called  $\alpha$ -level sets (Figure 5.2). All  $\alpha$ -level sets are crisp subsets of the support.

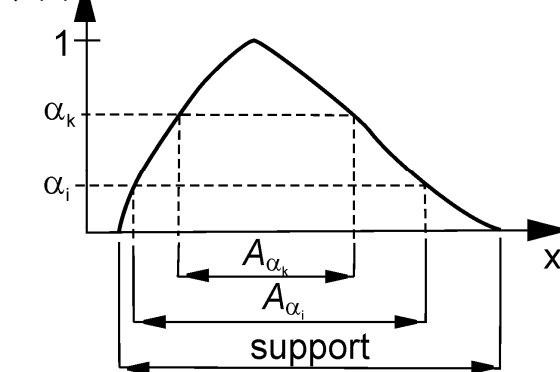


Figure 5.2 Support and  $\alpha$ -level sets

For several fuzzy quantities  $\tilde{x}_1, \dots, \tilde{x}_n$  on the fundamental sets  $\mathbf{X}_1, \dots, \mathbf{X}_n$  the *Cartesian product* can be determined. Thereby the product space  $\mathbf{X} = \mathbf{X}_1 \times \dots \times \mathbf{X}_n$  is formed, whose coordinate axes are perpendicular to one another. The Cartesian product  $\tilde{K}$  comprises all combinations of elements  $x_1, \dots, x_n$  of the  $\tilde{x}_1, \dots, \tilde{x}_n$ . The membership values

$\mu_K(\underline{x}) = \mu_K(x_1, \dots, x_n)$  of each n-tuple  $(x_1, \dots, x_n)$  is determined with the aid of the minimum operator  $\mu_K(\underline{x}) = \min_{i=1, \dots, n} [\mu(x_i)]$ . The Cartesian product  $\tilde{K}$  thus represents a n-dimensional fuzzy set in the product space  $\underline{X}$  with the membership value  $\mu_K(\underline{x})$ .

Determining  $\tilde{K}$  interaction between fuzzy quantities can be considered. *Interaction* is defined as being the mutual dependency of fuzzy quantities. An interactive relationship may be formulated directly (explicitly) or indirectly (implicitly). Directly formulated interactions are a priori given by means of functions which define constraints in the product space  $\underline{X}$ . These functions can be defined for several  $\alpha$ -levels differently. Against this, indirect formulated interaction occurs within the mapping of fuzzy quantities  $\tilde{x}_1, \dots, \tilde{x}_n$  onto fuzzy quantities  $\tilde{z}_1, \dots, \tilde{z}_m$ . If several  $\tilde{x}_i$  affect different results  $\tilde{z}_j$  simultaneously, these  $\tilde{z}_j$  are not longer independent of each other, i.e., interaction exists between them. The mapping model determines the functional relationship of this interaction.

To specify the membership function a general algorithm is not available. The obtained membership functions represent a subjective assessment reflecting actual facts. It is reasonable selecting simple functions to describe the membership function  $\mu(x)$ , e.g., linear or polygonal. Therefore, fuzzy triangular numbers  $\tilde{x}_T = \langle x_1, x_2, x_3 \rangle$  are frequently used which are determined by specifying the smallest and the largest value  $x_1$  and  $x_3$  (interval bounds of the support) as well as the value  $x_2$  belonging to  $\mu(x_2) = 1$ . Also linguistic variables can be utilized. Thereby, the term set  $T$  is mapped onto the fundamental set  $\mathbf{X}$  including the physically relevant numerical elements  $x \in \mathbf{X}$ . For example, the set  $T$  may comprise the terms *very low*, *low*, *medium*, *high*, and *very high*, which could assess the consequence of structural failure due to an earthquake.

If the fluctuation of an uncertain parameter depends on time or spatially coordinates, fuzzy functions may be defined. A *fuzzy function* of the form  $\tilde{x}(\underline{t})$  is the result of the uncertain mapping of the fundamental set  $\underline{T} \subseteq \square^n$  onto the set  $\mathbf{F}(\mathbf{X})$  of fuzzy quantities  $\tilde{x}$  belonging to the fundamental set  $\mathbf{X}$ . In earthquake analysis the multidimensional fundamental set  $\underline{T}$  may generally contain arbitrary coordinates  $\varphi$  beside the time  $\tau$  and the spatial coordinates  $\underline{\theta}$ . The values of  $\underline{\theta}$ ,  $\tau$ , and  $\varphi$  are combined in the vector  $\underline{t} = (\underline{\theta}, \tau, \varphi)$ . Thereby  $\underline{t}$  represents a vector in the parameter space  $\underline{T} \subseteq \square^n$ .

A frequently more efficient definition is given by

$$\tilde{x}(\underline{t}) = x(\underline{s}, \underline{t}) = \left\{ x(\underline{s}_j, \underline{t}), \mu(x(\underline{s}_j, \underline{t})) \right. \\ \left. \left| \underline{s}_j \in \underline{s}; \mu(x(\underline{s}_j, \underline{t})) = \mu(\underline{s}_j) \right. \right\}$$

the *fuzzy bunch parameter* representation of the fuzzy function  $\tilde{x}(\underline{t})$ .

Thereby  $\underline{s} = (\tilde{s}_1, \dots, \tilde{s}_{n_s})$  is the vector of fuzzy bunch parameters. To the components  $\tilde{s}_1, \dots, \tilde{s}_{n_s}$  of  $\underline{s}$   $\alpha$ -discretization is applied. The  $\alpha$ -level sets  $S_{1,\alpha}, \dots, S_{n_s,\alpha}$  result which are combined by means of the cartesian product. In that way they form the  $n_s$ -dimensional crisp subspace  $\underline{S}_\alpha$  for each  $\alpha$ . Analyzing elements  $\underline{s}_j \in \underline{S}_\alpha$  one obtains a crisp set of real-valued functions which is referred to as  $\alpha$ -function set

Any arbitrary function  $x(\underline{s}_j, \underline{t})$  contained in  $X_\alpha(\underline{t})$  is a *trajectory* of the fuzzy function on the level  $\alpha$ . In the case that all bunch parameters are fuzzy numbers, the trajectory for  $\alpha = 1$  is referred to as *trend function*. Based on the  $\alpha$ -discretization the fuzzy function  $\tilde{x}(\underline{t})$  is described as a set of  $\alpha$ -function sets  $X_\alpha(\underline{t})$  with the assigned membership value  $\mu(X_\alpha(\underline{t})) = \alpha$ . Furthermore, each of these  $\alpha$ -function sets  $X_\alpha(\underline{t})$  represents an assessed bunch of real-valued functions.

### 5.1.3 Fuzzy analysis

The analysis with certain (or uncertain) algorithms and with fuzzy quantities as input and model parameters is referred to as fuzzy analysis. Depending on the problem focused the fuzzy analysis is also referred to as fuzzy structural analysis or fuzzy earthquake analysis. The results of fuzzy analyses are also fuzzy quantities  $\tilde{z}_j$ . They depend on n fuzzy input variables  $\tilde{x}_i$  and p fuzzy model variables  $\tilde{m}_r$ .

Therefore,

- 1) all elements  $\underline{x}$  out of the space of fuzzy input variables  $\underline{x}$  have to be transformed into the space of fuzzy result variables  $\underline{z}$  and
- 2) the membership functions  $\mu(\underline{z})$  have to be determined.

The transformation  $\underline{x}$  to  $\underline{z}$  according to 1) is realized with the aid of the mapping  $\underline{z} = f(\underline{x})$ .  $f(\cdot)$  represents the deterministic model  $M$  of the fuzzy analysis. Fuzzy model variables  $\tilde{m}_r$  are included in the model  $M$  leading to an uncertain mapping  $\tilde{f} = \tilde{M}$ . In the analysis algorithm they are considered just like the fuzzy input variables  $\tilde{x}_i$ .

The determination of membership values  $\mu(z_j)$  of the elements  $z_j$  of the fuzzy result variables  $\tilde{z}_j$  according to 2) is feasible with several methods. The extension principle in combination with the Cartesian product of uncertain sets utilizes the max-min-operator. The application demands the discretization of the fuzzy input variables  $\tilde{x}_i$  in almost indefinitely points along the  $x_i$ -axes. This leads to numerical problems frequently. Therefore a method is required, which discretizes the axis of the membership values

$\mu$  - in contrast to the extension principle - and which does not presume special requirements of the mapping like linearity or monotonicity. The developed method, called  $\alpha$ -level-optimization, substitutes the max-min-operator of the extension principle, see Möller et al. 2000.

Thereby the concept of  $\alpha$ -discretization is adopted. All fuzzy input variables are discretized using the same number of  $\alpha$ -levels  $\alpha_k$ . For a certain  $\alpha_k$  the  $\alpha$ -level sets  $A_{i,\alpha_k}$  form the crisp subspace  $\underline{X}_{\alpha_k}$  by means of the Cartesian product. With the mapping  $\underline{z} = f(x_1, \dots, x_n)$  elements of the  $\alpha$ -level set  $B_{j,\alpha_k}$  of  $\tilde{z}_j$  may be computed on  $\alpha_k$ . The mapping of all elements of  $\underline{X}_{\alpha_k}$  yields the crisp subspace  $\underline{Z}_{\alpha_k} = B_{1,\alpha_k} \times \dots \times B_{m,\alpha_k}$ . Once the largest element and the smallest element of  $B_{j,\alpha_k}$  have been found, two points of the membership function  $\mu(z_j)$  are known. Repeating this for a sufficient large number of  $\alpha_k$  the functions  $\mu(z_j)$  are completely described in the case of convex fuzzy result variables.

In search of the largest element and the smallest element of each  $B_{j,\alpha_k}$  the  $\alpha$ -level-optimization requires the repeated solution of an optimization problem using general performance functions. A sophisticated optimization algorithm has to be efficiently, robustly and reliably. Because standard optimization algorithms are limited in application, a combination of evolution strategy, gradient method and Monte Carlo methods was developed as an agreement. This optimization method is referred to as *modified evolution strategy*.

When the mapping is stepwise applied, the interactive dependencies between intermediate results must be considered. Nonobservance of this interaction leads to the defect that, starting from the intermediate results, nonpermissible parameter combinations are generated and processed forward. Thereby additional, artificial uncertainty is introduced into mapping in each step (Möller & Beer 2004).

For mapping M any analysis algorithm can be applied. For example in structural mechanics geometrically and physically nonlinear fuzzy equations of motion:

$$\tilde{\underline{M}}(\tau) \cdot \Delta \tilde{\underline{v}}(\tau) + \tilde{\underline{D}}(\tau, v, d) \cdot \Delta \tilde{\underline{v}}(\tau) + \tilde{\underline{K}}_{\tau}(\tau, v, d) \cdot \Delta \tilde{\underline{v}}(\tau) = \Delta \tilde{\underline{P}}(\tau)$$

$\tilde{\underline{M}}$  fuzzy mass matrix       $\tilde{\underline{D}}$  fuzzy damping matrix

$\tilde{\underline{K}}_{\tau}$  tan gential fuzzy stiffness matrix       $\Delta \tilde{\underline{P}}$  incremental fuzzy load vector

$\Delta \tilde{\underline{v}}$  incremental fuzzy displacemant vector

$\tau$  time       $d$  discrete damage indicator  
represent the basis to compute displacements and further fuzzy result variables, e.g., stresses (Möller

et al. 2004). They can be solved by means of the *fuzzy finite element method* (Möller et al. 2001).

Evaluations of the fuzzy result variables are carried out e.g. with the aid of defuzzification. Further, the fuzzy results including all computed deterministic points  $\underline{z} = f(x_1, \dots, x_n)$  are utilized for a new structural design method based on clustering (Möller & Beer 2004).

## 5.2 Example: evaluation of the seismic response of a concrete frame

The concrete frame of Fig. 5.3 is considered that corresponds to an existing structure. The measurements obtained for the material properties of this structure gave the fuzzy number of Fig.5.4 for the steel and the concrete respectively. The beams of this system are loaded with a dead load of 30.0 kN/m and a live load of 15.0 kN/m. The structure is located in a seismic zone with the following characteristics: Spectral acceleration: 0.16g, Soil type: B, Effective damping: 5%, Importance factor: 1.00, Foundation factor: 1.00.

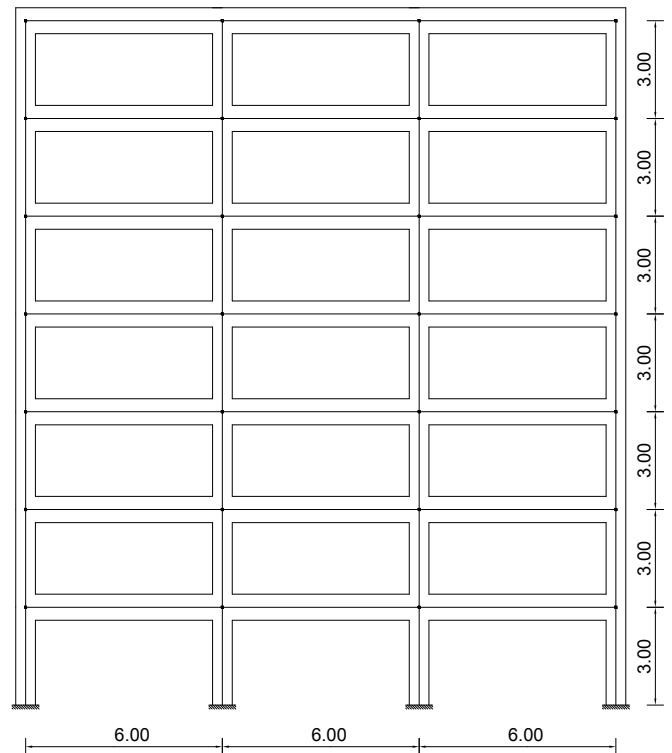


Figure 5.3 Seismic design of a concrete frame

In order to perform the elastoplastic analysis the following data are used.

- The amount of the upper (resp. lower) reinforcement of the beam cross section is equal to 8.0cm<sup>2</sup> (resp. 4.0cm<sup>2</sup>).
- The total amount of the column longitudinal reinforcement is equal to 20.24cm<sup>2</sup> and it is un-uniformly distributed along the perimeter of the column.

The objective is the determination of the structural response, which is expressed by the capacity curve and the value of the top-level horizontal displacement. It is expected that the variability in the material properties will result to different capacity curves. The structural calculations are performed using elastoplastic analysis and the seismic displacement is calculated according to the recommendations of FEMA356.

Fig. 5.5 presents the “fuzzy” capacity curve obtained by applying the  $\alpha$ -level-optimization algorithm. The vertical axis gives the ratio between the horizontal (H) and the vertical (V) loads applied on the structure. The various expected points of maximum seismic displacement are denoted with a box on these diagrams.

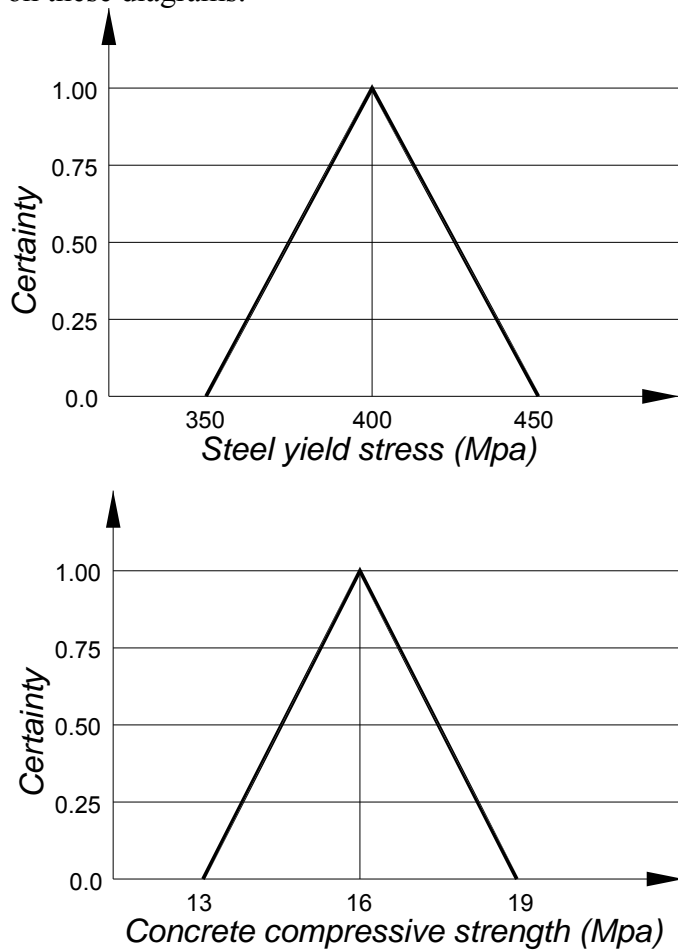


Figure 5.4 Fuzzy numbers for the steel yield stress and for the concrete compressive strength.

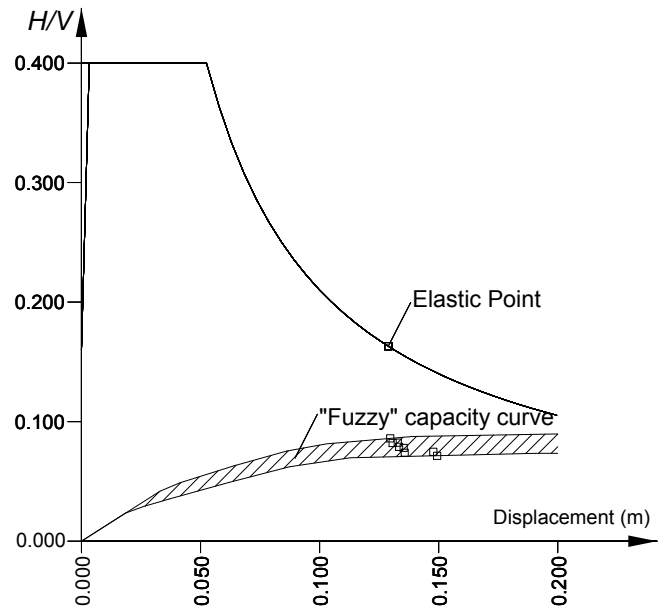


Figure 5.5 The obtained “fuzzy” capacity curve

The diagram of Fig. 5.6 is the fuzzy number of the top horizontal displacement. It is noticed that although the input parameters were triangular fuzzy numbers, the output parameters are not. This happens due to the strong nonlinearities involved in the static analysis. However, it is interesting to notice that although the ratio between the upper and lower values of the steel yield stress (resp. the concrete compressive strength) is equal to 1.29 (resp. 1.46), the ratio between the upper and lower value of the displacement is equal to 1.15, i.e. the variation of the output parameter is lower than that of the input parameters.

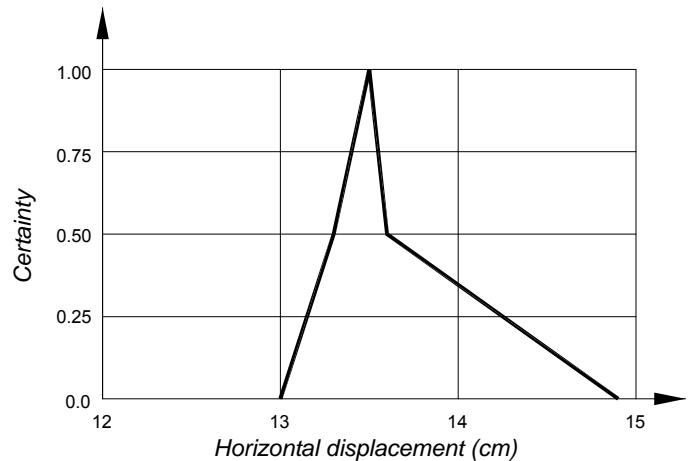


Figure 5.6 The obtained fuzzy number for the top horizontal displacement

## 6 PERFORMANCE BASED EARTHQUAKE ENGINEERING AS A TOOL FOR THE STUDY AND EVALUATION OF THE STRUCTURAL RESPONSE

### 6.1 Introduction

Exceptional seismic events are not only the result of uncertainty of the seismic motion, as was already clearly stated in the introduction. The nonlinear dynamic response of the structure also constitutes a crucial aspect that may result in exceptional consequences. This naturally reflects the complexity of the problem and the lag that still exists between standard engineering practice and the sophisticated and time-consuming approaches that would be required to narrow down the uncertainty associated with the currently accepted reliability targets.

Additionally, the built environment spans a few centuries and consequently exhibits a large scatter in terms of its compliance with current safety levels with respect to seismic actions that adds a third source of exceptionality.

Performance-based design is nowadays becoming the standard design methodology for the design of structures. This is a direct consequence of great theoretical and numerical advances in structural analysis, coupled with a higher “statistically” confidence in the characterization of design actions.

Following the discussion of nonlinear analysis methods in section 3 and the specific response of short-period structures of section 4, sub-section 6.2 highlights the relevant role of the connections in the seismic response of structures. An application of the influence of an exceptional seismic event is also illustrated. Section 6.3 and 6.4 present a capacity design methodology and a direct displacement-based design approach for the design and evaluation of the seismic resistance of reinforced concrete structures.

#### 6.2 Influence of connection behaviour on the seismic response of structures

The behaviour of steel or composite joints under seismic loading provides a good exemplification of the issues discussed in the previous sub-section. Usually, seismic events provoke relatively high amplitudes of rotation in the joint area, so that steel repeatedly reaches the plastic range and the joint fails after a relatively small number of cycles.

For static monotonic situations it is nowadays possible to accurately predict the moment-rotation response of a fairly wide range of joint configurations by applying the principles of the component method (Eurocode 3, 2005; Jaspert, 2000). However, this is still not the case for the cyclic situation. In this case,

the usual approach is to develop multi-parameter mathematical expressions that are able to reproduce the range of hysteretic behaviours for a given group of steel joint typologies. Subsequently, the values of the parameters are calibrated to satisfactorily correlate to a range of section sizes for a given group of joint typologies.

Mazzolani (1988) developed a comprehensive model based on the Ramberg-Osgood expressions that was able to simulate the pinching effect, later modified by Simões et al. (2001) to allow for pinching to start in the unloading zone. The Richard-Abbott expression was first applied to the cyclic behaviour of joints by De Martino et al. (1984). Unfortunately, that implementation was not able to simulate the pinching effect (Simões et al., 2001). Subsequently, Della Corte et al. (2000) proposed a new model, also based on the Richard-Abbott expressions, that was capable of overcoming this limitation and simulate the pinching effect, as well as strength and stiffness deterioration and the hardening effects.

Since the mid 1980's, several research projects on the cyclic behaviour of steel joints were undertaken in various research centres, comprising a total number of 39 research projects and 216 individual experimental tests. In general, the objective of these cyclic tests was the study of the seismic performance of the joints, following the observation of failures resulting from the Kobe and Northridge seismic events.

#### 6.2.1 The influence of pinching

The influence of pinching is crucial in the establishment of the model parameters. For the end-plate joints, this is clearly noticeable and it is necessary to establish whether pinching is likely to occur. Its influence is illustrated using three steel structures, two plane frames and a three dimensional structure. The first structure is a low rise office building with four spans and two floors, the second structure has two spans and five floors, and finally the third is a 3D structure, with four by five spans and eight floors, using both non-linear static and dynamic analyses. The mathematical model consists of beam elements, for the beams and columns, and of joint elements, to model the non-linear behaviour of the connections. The numerical studies were performed with the SeismoStruct program (Seismosoft 2004), which has a specific joint element to model the connections. For this element several parameters have to be defined to characterize all non-linear hysteretic behaviour (Nogueiro *et al.* 2005).

For the 3D structure the floor diaphragms are assumed to be rigid in the horizontal plane. For this structure the study was performed only for the strong axis direction. For all structures a 2% damping coefficient was considered. The first 2-D struc-

ture, herein called E-2x4-2D is a low rise office building, with four spans and two floors, as can be seen in the Figure 6.1.

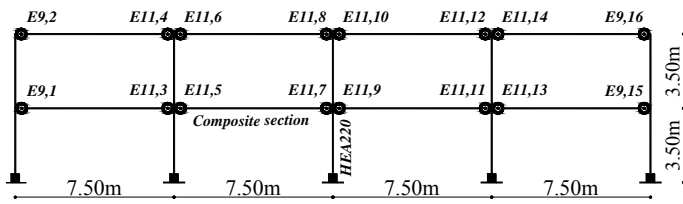


Figure 6.1. Geometry of the structure E-2x4-2D. The connections considered to this structure present the hysteretic behaviour of Figures 6.2 and 6.3, respectively for external E9 and internal E11 connections.

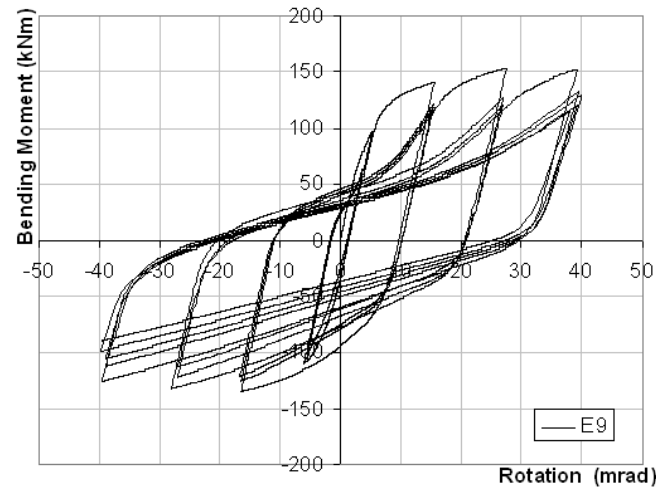


Figure 6.2. Hysteretic curve for external E9 connection.

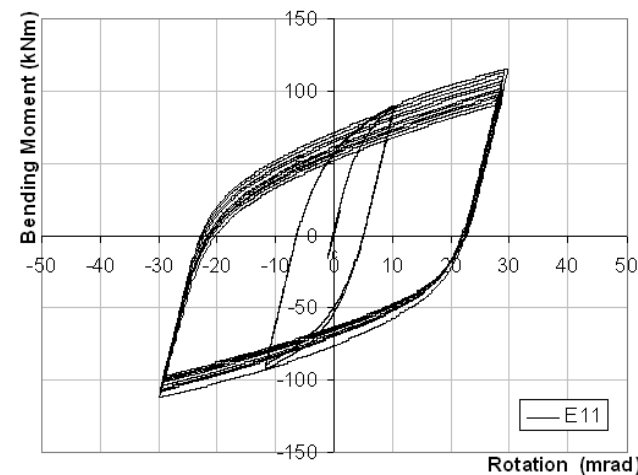


Figure 6.3. Hysteretic curve for internal E11 connection

The second structure studied, E-5x2-2D, (Della Corte *et al.* 2000), is also a 2D structure, with two spans and five floors, as can be seen in Figure 6.4. The behaviour of the connections was idealised, according to the JB1-3A connection (Bursi *et al.* 2002) and the corresponding parameters are presented in (Nogueiro *et al.* 2005).

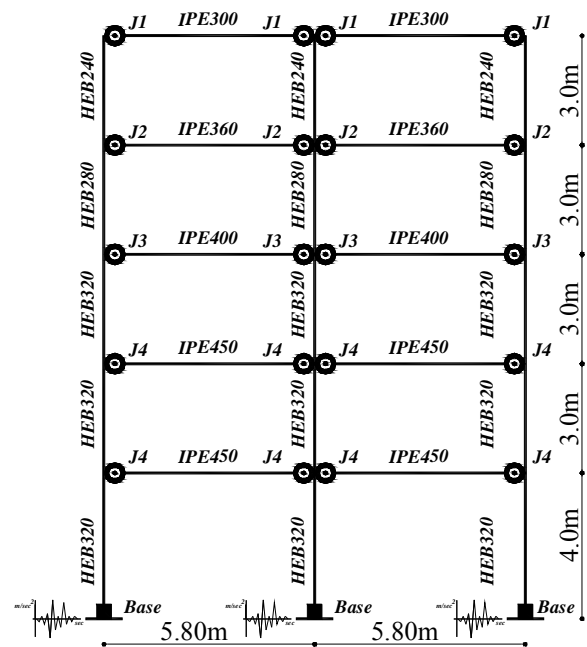


Figure 6.4. Geometry of the structure E-5x2-2D

The third structure, E-4x5x8-3D, is three dimensional with four by five spans and eight floors, as represented in Figures 6.5 and 6.6. It corresponds to a real structure existing in Cardington, England, modified to match Eurocode 8 requirements for Portugal (Nogueiro *et al.* 2005).

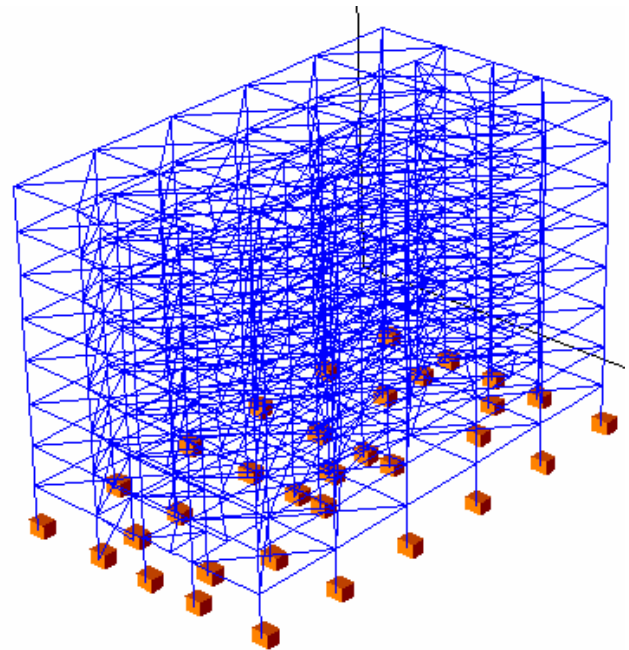


Figure 6.5. Three-dimensional view of E-4x5x8-3D.

The structures were designed according to Eurocode 8 for a soil type B (medium soil) response spectrum, for a given design q factor (reduction factor) and assuming a given ductility class. Linear dynamic analyses of the structures were carried out, and the design action effects were calculated adding the gravity and the seismic effects divided by the assumed q factor.

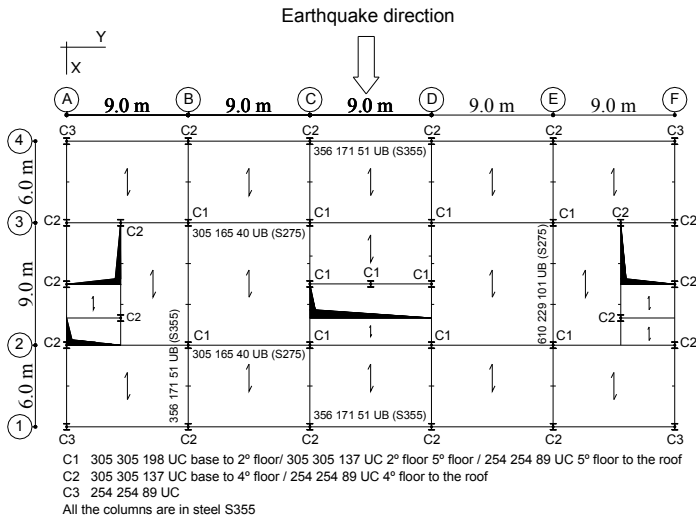


Figure 6.6. Plan of one inter storey.

In the design procedure dead and live loads were considered and the seismic action was represented by the acceleration response spectrum (Nogueiro et al, 2006). For the non-linear dynamic analyses the designed structures have to be subjected to, at least, three accelerograms (#1, #2 and #3), compatible with soil type B response spectrum (Eurocode 8 2003). A large number of accelerograms compatible with the target response spectrum were generated. The three having the best fit to the target response spectrum were chosen. These accelerograms are different from real earthquake records, given that their target response spectrum is a smooth one. Anyway, they are in accordance with the seismic action that was assumed for design purposes and which is the one considered as most likely to occur, mainly in the range of periods between  $0.2 T_1$  and  $T_1$  as it is specified in the Eurocode 8 ( $T_1$  represents the fundamental period). Figure 6.7 presents the three response spectra corresponding to the three chosen accelerograms together with the target (Eurocode 8) response spectrum. Figure 6.8 illustrates one of the accelerograms chosen.

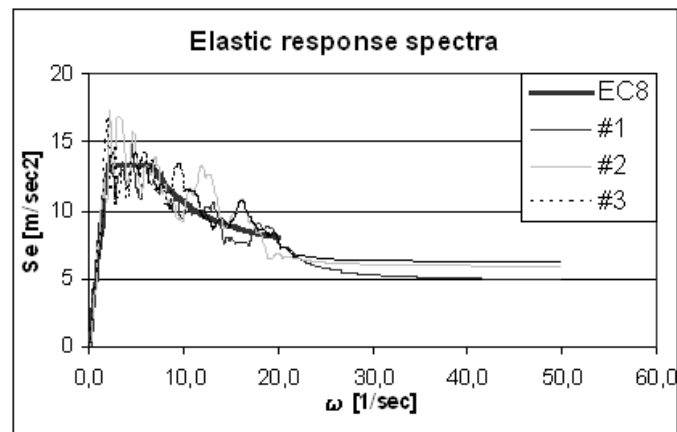


Figure 6.7. Elastic response spectra,  $\xi = 2\%$ .

For the non-linear dynamic analyses, three combinations of loads were considered, one for each accelerogram. The 3D structure was subjected only to

seismic action acting in X-direction, as can be seen in Figure 6.6.

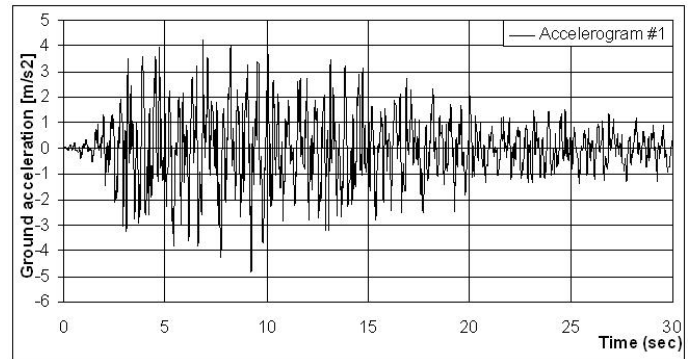


Figure 6.8. Artificial accelerogram.

The seismic assessment of three steel structures is performed by means of non-linear static analyses (the N2 method (Fajfar, 2000) was adopted) and the results obtained are compared with the ones obtained with non-linear dynamic analysis. The SeismoStruct program (Seismosoft, 2004) was used for all the numerical studies. Some conclusions could be reached regarding the non-linear static analysis, the structures and the results obtained:

- It is observed a good agreement between the nonlinear static and dynamic analyses, in particular in terms of the horizontal displacements and inter-storey drifts results;

- The first structure studied (E-2x4-2D) needs to be redesigned or retrofitted; as the seismic demands values are above the correspondent capacity values, however, it is noted that the reference seismic event exhibit an extreme value of peak ground acceleration ( $0.45g$ ), 50% in excess of the usual reference earthquake for Portugal.

- The other two structures, E-5x2-2D and E-4x5x8-3D, exhibit overstrength, considering the horizontal displacements values and the maximum rotation values at the connections;

- The model to simulate the hysteretic connection behaviour for the non-linear dynamic analysis presents good results;

- The N2 method seems to be a conservative design procedure, when compared with the dynamic analysis.

Table 6.1 presents the maximum rotation in the connections analysed, for the several methods. For structure E-2x4-2D, where the horizontal top displacements are almost the same, the rotations are larger in the dynamic analysis. The monotonic method does not include the effect of pinching, and damage of strength and stiffness. In the second structure, where the horizontal top displacements, in the N2 method are larger than in the dynamic analysis, the rotation in the J231E/J4 connection is almost the same, and finally, in the third structure, where the horizontal top displacement in monotonic method is significantly larger than in dynamic analysis,

it is showed that in J53EF/J-X610 connection the rotation is smaller for the dynamic analysis, as expected. It can be concluded that, for study of the behaviour of the connections, the monotonic methods have some limitations, because they give insufficient hysteretic information.

Table 6.1. Maximum rotation in the analysed connections.

Connections	rot. (mrad) dynamic	rot. (mrad) N2 (uniform)	rot. (mrad) N2 (modal)
E 9,15	48.0	27.6	30.2
E11,7	46.3	30.4	33.3
J231E/J4	15.7	13.9	15.8
J53EF/J-X610	8.8	16.9	20.3

### 6.2.2 Comparative effect of extreme event

For a steel structure with 8 stories, the influence of the connections simulated with semi-rigid behaviour and partial strength are compared with rigid behaviour and fully strength, for an extreme seismic event, for the Portuguese territory, using a pushover analysis. The structure chosen can be observed in Figure 6.9. The columns and beams are, respectively HEA320 and IPE260 sections. Two analyses were performed, one considering the connections semi-rigid with the real behaviour and other one considering the connections totally rigid with full strength.

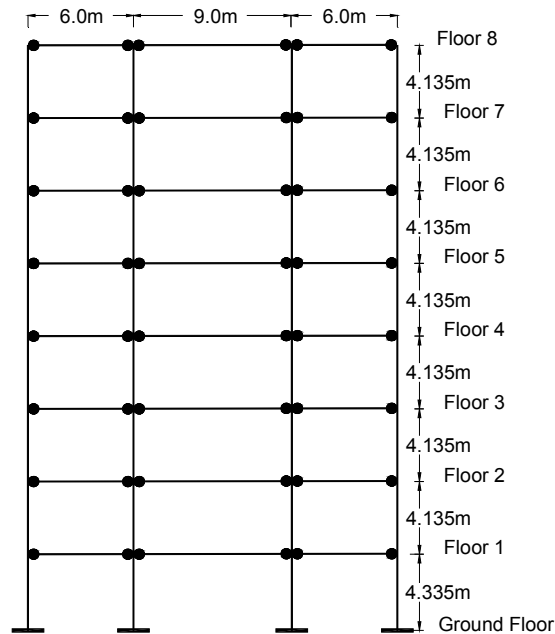


Figure 6.9. Geometric definition of the structure



Figure 6.10. Typical connection.

The results were obtained using the N2 method (Fajfar 2000) and are presented in terms of horizontal displacements, inter-storey drifts and rotations at the connections. The spectrum is graphically represented in ADRS format (Acceleration Displacement Response Spectrum), Figure 6.11, where the acceleration spectral values are defined as a function of the spectral displacement values. It represents an extreme event for Portugal, which means two times of the maximum spectral values for seismic type 2.

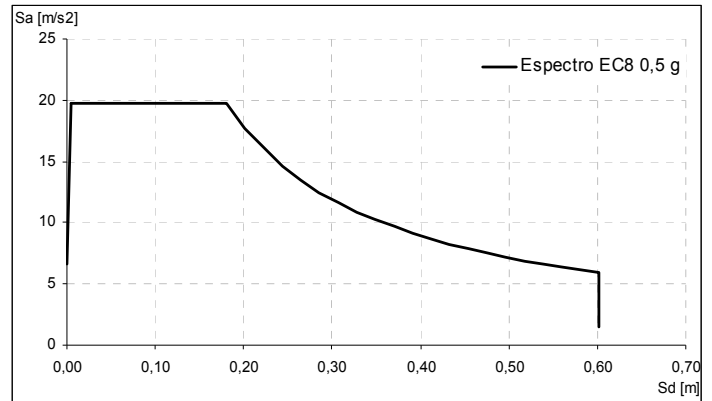


Figure 6.11. Response Spectrum in ADRS format,  $\xi = 2\%$ .

After defining of the action, it is needed to calculate the eigenvalues to assess the dynamic properties of the structure. These properties are important to transform the real structure in an equivalent simple degree of freedom system (SDOF), because the action it was defined by mean of response spectrum for a SDOF system, as it was presented. The capacity curve of the real structure, found it by means of that lateral load pattern (that can be uniform, triangular or a modal distribution) must be transformed of equivalent SDOF system. In Figures 6.12 and 6.13 the capacity curve for the equivalent SDOF can be observed, respectively for the structure with semi-rigid connections and rigid connections, and the respective bi-linearization.

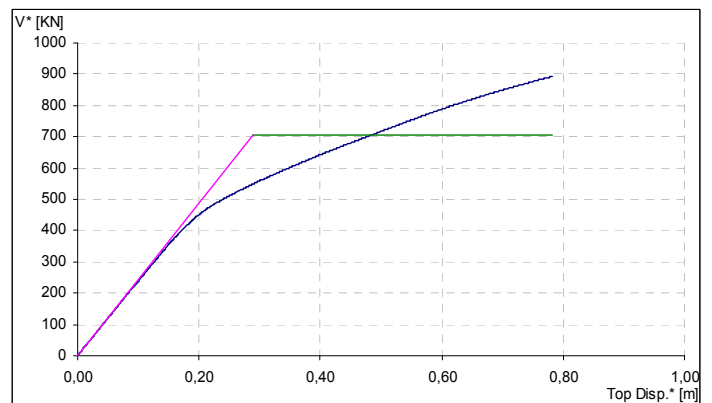


Figure 6.12. Structural Capacity Curve with semi-rigid connections.

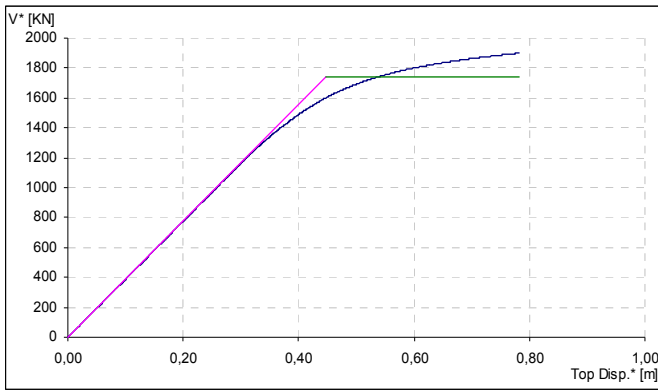


Figure 6.13. Structural Capacity Curve with rigid connections.

The bi-linearization curve must be put into the response spectrum (seismic action) and determine the target displacement, which represents the maximum top displacement for the actions considered. This procedure can be seen in Figures 6.14 and 6.15, respectively for the structure with semi-rigid and rigid connections. In the case of the first structure the behaviour it is clearly non linear, while in the second the structural behaviour remains elastic.

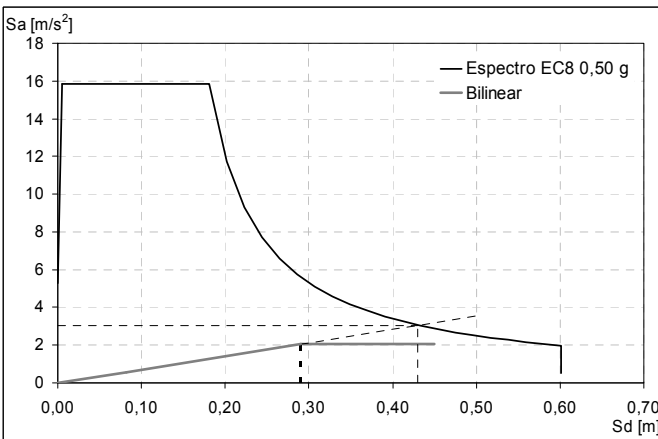


Figure 6.14. Target displacement for the structure with semi-rigid connections.

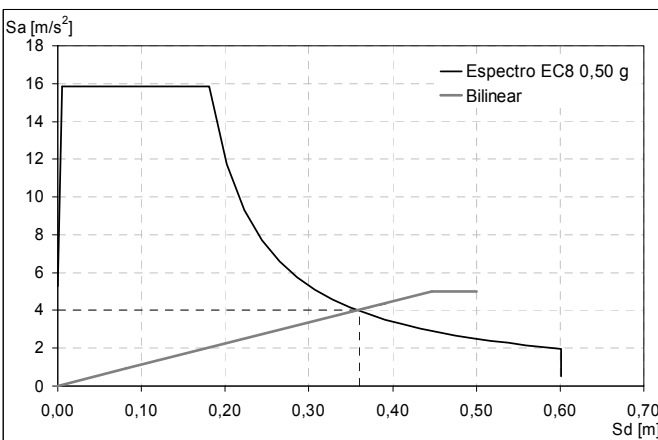


Figure 6.15. Target displacement for the structure with rigid connections.

If the real structures were reloaded until the target displacements, the maximum horizontal displacements

(Figure 6.16) and the inter-storey drifts (Figure 6.17) illustrate the differences between both simulation, and the influence of the semi-rigid connection behaviour.

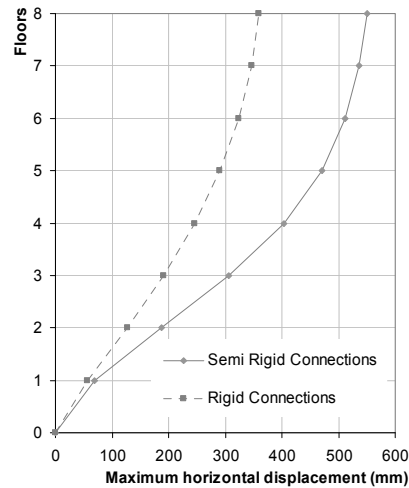


Figure 6.16. Maximum horizontal displacements.

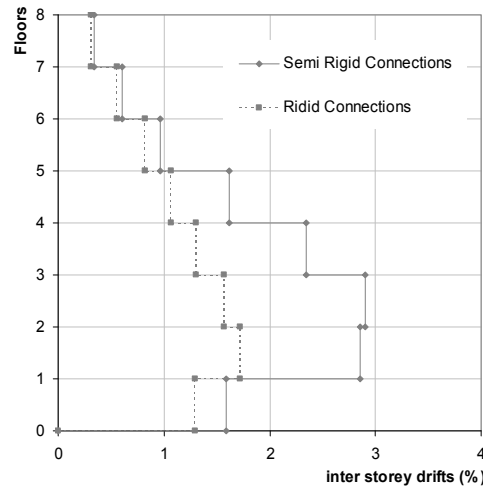


Figure 6.17. Inter storey drifts.

Despite the magnitude of the seismic event, the maximum horizontal displacement reached for the structure with semi-rigid connection was 55 cm, lower than 2,5% of the total height of the building and the rotation of the connection more stressed was approximately 22 mrad, which represent values lower than the ultimate strength values (Figure 6.18).

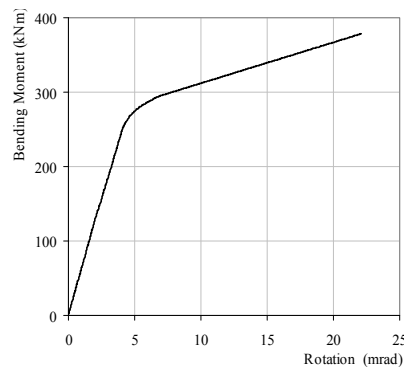


Figure 6.18. Bending-moment rotation for the most stressed connection.

### 6.3 *Capacity design methodology for design and evaluation of seismic resistance of RC building structures*

The Institute of Earthquake Engineering and Engineering Seismology, IZIIS in Skopje has developed a methodology and a corresponding package of computer programmes, RESIST-INELA for design of new and evaluation of seismic resistance of existing R/C building structures. The methodology is iterative until defining optimal structural system. The methodology incorporates the latest knowledge gathered in our country and the worldwide experience from the field of earthquake engineering: determination of strength and deformability characteristics of buildings, on one hand, and definition of the nonlinear behaviour of the structure for a given earthquake, on the other hand. This methodology has been used for design of a great number (more than 150) R/C building structures constructed in the territory of the city of Skopje.

#### 6.3.1 *Philosophy of capacity design*

Procedures for the application of capacity design to ductile structures, which may be subjected to large earthquakes, have been developed primarily in New Zealand over the last 20 years.

The main idea of this method is to predetermine places at which the occurrence of nonlinear deformations shall be dictated. These critical parts, the so called plastic hinges, are designed and processed separately to enable those places dissipate the total energy. It is desirable that all the inelastic deformations be due to bending, which with the provided previous and necessary conditions, corresponds to ductile behaviour of the structure.

Also, sufficient bearing capacity is provided for the remaining parts of the structure in order that they remain in the elastic range of behaviour during the whole earthquake action so that there is no need for their ductility.

#### 6.3.2 *Method for design and seismic evaluation of RC buildings developed at IZIIS, Skopje*

The definition of a method for design and evaluation of the seismic resistance of R/C building structures is a wide and complex problem. One hand, it is necessary to carry out the most possible realistic definition of the structural system capacity, in terms of strength and deformability capacity of the system, and on the other hand, after having selected the expected earthquake effect on a given site, in terms of intensity, frequency content and time duration, to predict as realistically as possible the nonlinear behaviour of the structure, and on the basis of these results to define the earthquake, i.e., the seismic force

or the acceleration that would cause damage to structural elements and the integral structural system.

For this purpose, it is necessary to develop a clear and concise procedure that will enable a fast and simple way for coming to the desired results. As a result of the analytical studies, carried out at IZIIS, Skopje, a method and a corresponding package of computer programmes RESIST-INELA, (Necevska-Cvetanovska, 1999) have been developed for a fast and simple evaluation of the seismic resistance of the newly designed and existing reinforced concrete buildings of small and moderate number of stories. The developed method is "capacity based" and incorporates the latest knowledge gathered in our country and the world experience from the broad fields of the earthquake engineering.

The method for evaluation of the seismic resistance of RC buildings, developed at IZIIS, consists in the following five steps:

- 1 Definition of the structural system of the building and determination of the quantity and quality of the built-in material.
- 2 Determination of the Q- $\Delta$  diagram for each element, separately, and the storey Q- $\Delta$  diagrams (RESIST-computer program).
- 3 Definition of the seismic parameters and the design criteria.
- 4 Nonlinear dynamic analysis of the structural system for a given earthquake effect (INELA-computer program).
- 5 Evaluation of the seismic resistance for the given structure.

##### 6.3.2.1 *First step*

The initial step for evaluation of the seismic resistance of a building is the definition of the structural system of the building as well as the quantity and the quality of the built-in material. The main information on the building, such as the structural type, number of stories, kind, quantity and quality of built-in material can be obtained from the design documentation for the considered building. For older buildings, it is possible that no design documentation is available. In such a case, the building is inspected for an in situ determination of the quantity and the quality of the built-in material. Elastic analysis of the structure is carried out under defined vertical loads and seismic forces.

Using a special data file, the quantity and the quality of the used steel reinforcement for each structural element cross sections (columns, walls and beams) are entered.

##### 6.3.2.2 *Second step*

The strength and deformability characteristics of each structural element of the building are defined applying the RESIST computer program, by which, starting with the elastic analysis of the structure and

the known quantity and quality of the built-in reinforcement and the achieved compressive strength of the concrete in all the cross sections of the elements (columns, beams and walls), for each storey element, separately, it is possible to obtain the yield displacement  $\Delta_y$ , the shear force at yielding  $Q_y$ , the maximum displacement  $\Delta_u$ , the shear force at maximum displacement  $Q_u$ . At the same time, the shear strength of each element of the building is determined taking into consideration that no shear failure of the element occurs. Summarizing  $Q-\Delta$  diagrams for each element at given level, storey  $Q-\Delta$  diagrams are obtained which represent the basis for further-nonlinear dynamic analysis of the building.

### 6.3.2.3 Third step

On the basis of the actual and the local site properties, applying probability methods, evaluation of the seismic hazard parameters is carried out according to which expected maximum ground accelerations for 50, 100, 200 and 500 year return periods are possible to be defined.

### 6.3.2.4 Fourth step

Nonlinear dynamic analysis of the structure modelled by lumped masses at floor levels for a given earthquake effect is performed. The application of different hysteretic models depending on the structural type and obtaining responses for a large number of ground acceleration time histories, with different frequency content and duration is possible for relatively short time and with the satisfactory accuracy.

### 6.3.2.5 Fifth step

The results obtained in the fourth step (relative storey drifts) are entered in the storey  $Q-\Delta$  diagrams, i.e., in the  $Q-\Delta$  diagrams for each structural element, from where is obvious which earthquake record and intensity can cause the occurrence of initial cracks, yielding and even failure of the structural elements of the building. The evaluation of the seismic resistance of the considered building can be defined by comparison of the nonlinear response "requirements" of the building to the given earthquake effect with the ultimate "capacity" of the building. The best indicator for these "requirements" and "capacity" is displacement.

### 6.3.2.6 Application of methodology on existing building B-2, Unit 4, "Vardar" settlement, Skopje

The 8 storey building is situated in Vardar settlement, (Simeonov et al. 1993) with previously defined seismic parameters as follows: maximum ground accelerations of 0.28g and 0.40g for the design and the maximum level. The structural system of the building consists of bearing RC frames in both directions (Fig. 6.19).

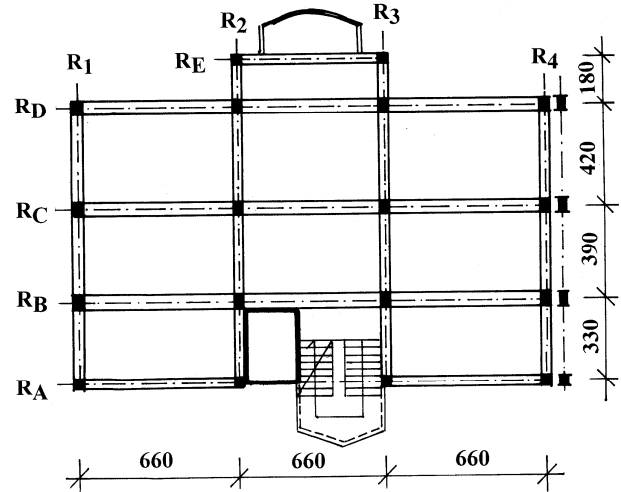


Figure 6.19 Characteristic plan of building structure.

Presented for the structure are the results from the design according to national regulations, (SP-81), EC8, (Eurocode 8, 1994) and the analysis performed by RESIST-INELA methodology, (Necavska-Cvetanovska & Gjorgjievaska, 1998), (Fig. 6.20).

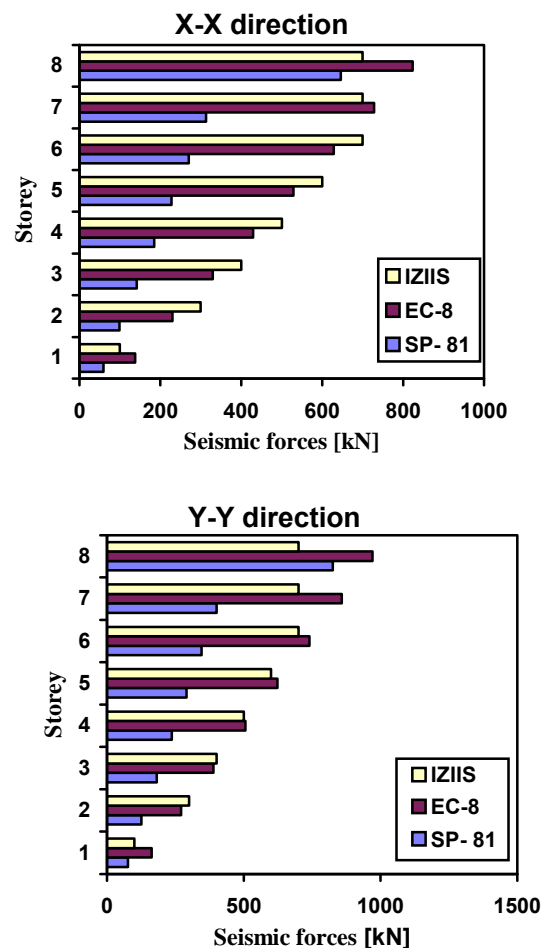


Figure 6.20 Seismic forces obtained according to SP-81, EC8 and IZIIS methodology.

Based on the adopted reinforcement, the bearing capacity and dynamic response of the structure

proportioned by these three different forces was defined, (Necevska-Cvetanovska & Petrusavska, 1996, 2000).

Tables 6.2 and 6.3 as well as Figure 6.21 show required displacement and ductility for the building designed according to SP-81, EC8 and IZIIS methodology for the Ulcinj (Albatros) earthquake of 0.4 g.

Table 6.2. Required displacements [cm], x-x direction.

Storey	SP-81	EC8	IZIIS
8	0.76	1.08	1.32
7	1.10	1.11	1.34
6	1.51	1.37	1.48
5	1.77	1.52	1.59
4	1.83	1.53	1.55
3	2.05	1.54	1.47
2	1.76	1.44	1.31
1	1.31	1.10	1.06

Table 6.3. Required displacements [cm], y-y direction.

Storey	SP-81	EC8	IZIIS
8	0.51	1.01	1.57
7	0.78	1.04	1.44
6	1.16	1.29	1.56
5	1.52	1.49	1.70
4	1.73	1.55	1.74
3	1.77	1.52	1.63
2	1.47	1.26	1.35
1	1.33	1.09	1.30

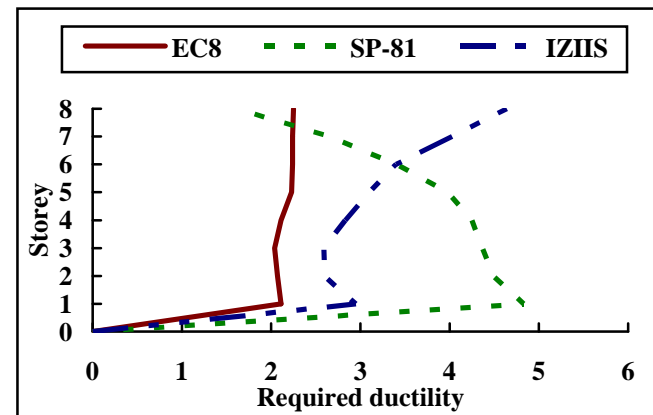


Figure 6.21 Required ductility, x-x direction.

#### 6.4 Direct displacement-based design approach for design of RC frame building structures

Modern trends in earthquake engineering show that there is a common consensus that the new design methodologies should be performance-based. Most of the currently used performance-based procedures are essentially force-based, with the addition of a displacement check to ensure that acceptable performance levels are achieved in the design earthquake. Displacement-based design procedure enables structures to be designed in way to respond in the design-level earthquake to specified displacement limits, corresponding to acceptable damage limit states. A direct displacement-based procedure for seismic design of RC building structures is presented. This design procedure uses the Substitute

Structure Approach. Based on the defined target displacement, the base shear demand is calculated and a structural design to resist this demand is performed. The next step is application of the capacity design approach and checking of the structural behaviour by nonlinear static analysis. The design is corrected, if necessary.

##### 6.4.1 Direct displacement-based design

The brief overview of the history of seismic design shows that the main design criteria in all the seismic regulations are those referring to strength, i.e., force. The huge economic losses from the recent earthquakes show that the current design methodologies fall short of realizing the goals and the objectives of the earthquake resistant design philosophy. Modern earthquake engineering increasingly points to the adequacy of displacement as a design parameter.

An alternative design procedure known as displacement-based design has been developed that attempts to recognize deficiencies in the current force-based approaches. Displacement-based seismic design is defined broadly as any seismic design method in which *displacement-related quantities* are used directly to judge performance acceptability. In the recent years, numerous displacement-based methods have been proposed. Some of them can be considered as true displacement-based methods, often named “direct displacement-based”, while the other are still “force-based/displacement-check” methods, although named displacement-based. The most developed and the most important method in the field of direct displacement-based design of RC building structures is the Priestley’s method, (Priestley, 2000, 2002).

Priestley’s direct displacement-based design, (DDBD) characterizes the structure by secant stiffness  $K_e$  at maximum displacement  $\Delta_d$ , (Fig. 6.22) and a level of equivalent viscous damping appropriate to the hysteretic energy absorbed during inelastic response. The approach used to characterize the structure is based on the “substitute structure” analysis procedure, (Shibata & Sozen, 1976).

With the design displacement  $\Delta_d$  determined and the damping estimated from the expected ductility demand, the effective period  $T_e$  at maximum displacement response can be read from a set of design displacement spectra, as shown in Fig. 6.22(d). Representing the structure (Fig. 6.22(a)) as an equivalent SDOF oscillator, the effective stiffness  $K_e$  at maximum response displacement can be found by inverting the equation for the natural period of the SDOF oscillator, namely:

$$T_e = 2\pi * \sqrt{\frac{M_e}{K_e}} \quad (6.1)$$

to provide

$$K_e = \frac{4\pi^2 m_e}{T_e^2} \quad (6.2)$$

where  $m_e$  is the effective mass.

From Figure 6.22(b), the design shear force at maximum response is:

$$V_b = K_e \Delta_d \quad (1.3)$$

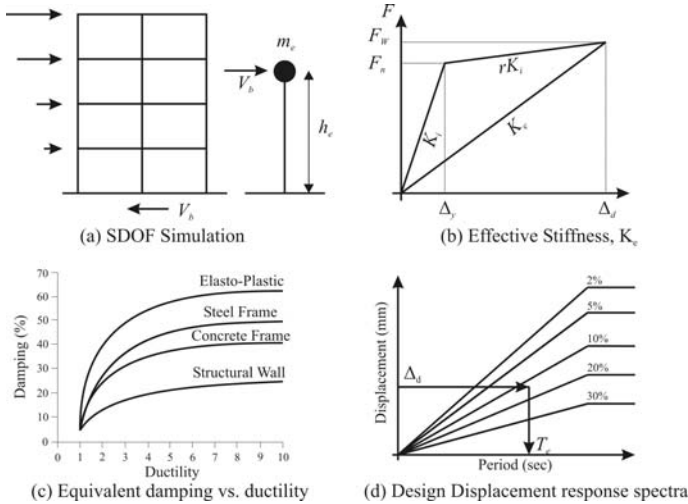


Figure 6.22 Fundamentals of Direct Displacement – Based Design, (Priestley, 2000, 2002).

#### 6.4.2 Application of DDBD approach – Design example

In order to determine the effort needed for direct displacement-based design of a RC frame building, an example structure is designed using the Priestley's method (Priestley, 2000, 2002) with minor changes that do not affect the essence of the original. Later, an example structure is analyzed using a non-linear static procedure, (Terzic, 2006).

The example structure is a 7 storey RC frame building. In order to simplify the calculations, it is assumed to be symmetric in both directions, wherefore the design and the analyzes are performed for one direction only. The building is square 25x25 m in plan with 5 m beam spans. Each storey has the same height of 3 m. The columns are assumed to be 60x60 cm for the first three stories, and 50x50 cm for the upper stories. All beams are assumed to be 30 cm wide and 50 cm deep, and in the calculations, they are treated as T or L beams, considering that a 20 cm deep slab is acting as a beam flange. For the purpose of the design, it is adopted that the compressive strength of concrete is  $f_c=35$  MPa, and the reinforcement yield stress is  $f_y=400$  MPa. The layout of the structure is given on Figure 6.23.

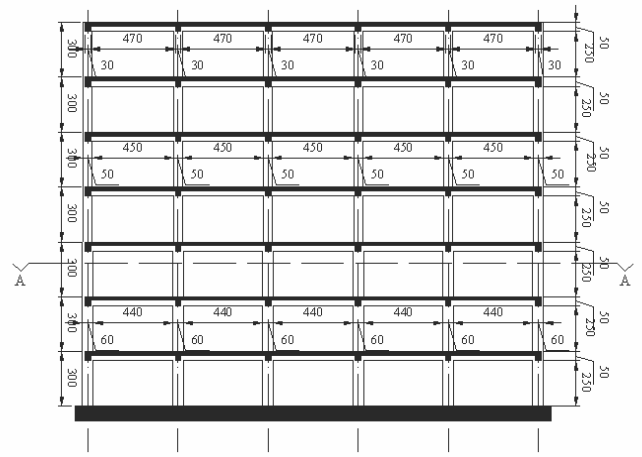


Figure 6.23 Cross-section of the example structure. The flowchart of the method is given in Figure 6.24.

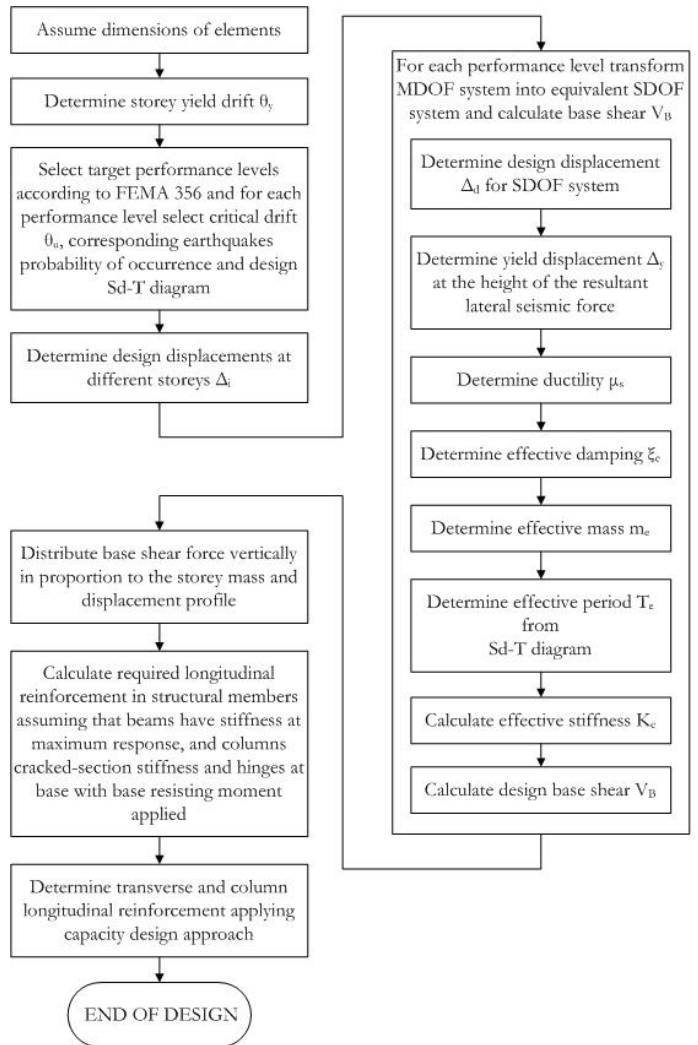


Figure 6.24 Flowchart of the applied method, (Priestley, 2000, 2002).

The design process consists of two parts: the first part in which the base shear force for each performance limit state is derived, (Table 6.4) and the second part in which that force is distributed over the structure and the required reinforcement is calculated, (Necevska-Cvetanovska&Petruševska, 2000).

Table 6.4 Design results

Earthquake	$\theta_y$	$\theta_d$	$\Delta_d$	$\Delta_y$	$\mu$	$\xi$
	(%)	(%)	(m)	(m)		
20%/50 years	0.01	0.01	0.139	0.15	0.92	3.81
10%/50 years	0.01	0.02	0.278	0.15	1.85	12.94
2%/50 years	0.01	0.04	0.555	0.15	3.70	19.40

Table 6.4 Design results - continued

Earthquake	$m_e$	$T_e$	$K_e$	VB
	(kg)	(s)	(kN/m)	(kN)
20%/50 years	3704984	2.65	20828.32	2890.59
10%/50 years	3704984	6.01	4049.46	1123.98
2%/50 years	3704984	6.50	3461.94	1921.81

In order to compare the capacity of the structure with the design demand, Static Nonlinear Analysis according to FEMA 356, (ASCE, 2000) was performed using the SAP 2000 software, (Wilson & Habibullah, 1998). Each beam was modeled with a plastic hinge at both ends. The columns were considered to behave linearly except at the base where plastic hinges were expected to occur. Same distribution of base shear was used as for the design. Gravity load consisting of dead and 50% of live load was applied on the structure prior to the pushover and the P- $\Delta$  effect was considered.

Different structural performance levels of plastic hinges are defined by FEMA 356 recommendations, but in order to achieve realistic performance of the structure, plastic hinges are modeled according to load-deformation relations obtained by analysis of each cross section using cross section analysis software XTRACT, (Imbsen Software Systems) rather than according to prescribed and extremely conservative relations given in FEMA document. Plastic hinge is considered to achieve Immediate Occupancy performance level when reinforcement yielding starts or concrete strains reach 0.003. Life Safety is associated with beginning of spalling of reinforcement cover and Collapse Prevention with significant strength degradation.

The results of the pushover analysis are presented in Tables 6.5 and 6.6 and Figure 6.25.

Table 6.5 Analysis results for target drifts (DDBD)

Earthquake	Drift (%)	Percentages of members achieving state		
		IO	LS	CP
20%/50 years	0.42	39	0	0
10%/50 years	0.61	66	0	0
2%/50 years	1.43	100	0	0

Table 6.6 Analysis results for target drifts (EC8)

Earthquake	Drift (%)	Percentages of members achieving state		
		IO	LS	CP
20%/50 years	0.39	2	0	0

10%/50 years	0.66	61	0	0
2%/50 years	1.25	100	0	0

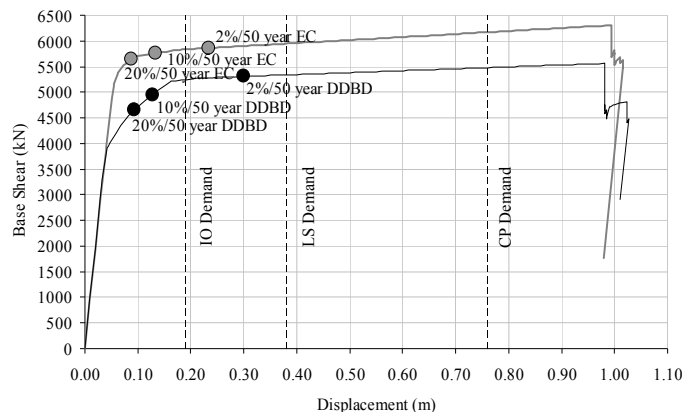


Figure 6.25 Pushover curves for building designed according to DDBD and EC8.

### 6.4.3 Remarks

- Seismic resistant design has radically been modified in recent years, by changing its philosophy from “strength” to “performance”. Most of the currently used performance – based procedures are essentially force-based, with addition of displacement check to ensure that acceptable performance levels are achieved in the design earthquake.
- Displacement-based design, as an alternative approach is based on design to achieve a specified strain or drift performance level under a specified seismic intensity. The approach should result in uniform levels of seismic risk and in more consistent designs than force-based design criteria.
- The initial design parameter of displacement-based design is target displacement. Strength and stiffness are a result of the design procedure and are dependent on the target displacement chosen. Nevertheless predicting target drift or yield displacement is not that simple, as it might seem at first.
- Direct displacement-based design, in every sense, coincides with actual structural behavior. It is, therefore, realistic to expect that this approach will soon find its place in most advanced building codes and that this philosophy of structural design will, in not so far future, replace currently established design procedure.
- In order to determine the effort needed for direct displacement-based design of a RC frame building, an example structure is designed using this method and latter analyzed using a nonlinear static procedure. It is concluded that, from the aspect of drift, the structure behaves satisfactorily, meaning that the target drifts for different hazard levels are smaller than the demand drifts.

## 7 CONCLUSIONS

The paper presented various ways in which the seismic action may be exceptional for structures. Pa-

parameters related to the ground motion were examined as well as parameters more closely related to the structure itself. Also, a mathematical framework based on fuzzy analysis was introduced allowing the consideration of the various uncertainties and their effects to the structural response. Finally, applications of the performance based engineering (PBE) were presented. In these applications PBE was used as a tool for the study of the influence of various parameters to the structural response and also for the evaluation and design of structures. It should be noticed that PBE can be used as a tool to adapt the "supply" of the structure (considering in this respect any particularities that it might have) to the specific "demand" of the motion, according to the importance of the building and the desired safety level.

## REFERENCES

- Ambraseys, N., Smit, P., Berardi, R., Rinaldis, R., Cotton, F., Berge-Thierry, C. (n.d.) "Internet-Site for European Strong-Motion Data", accesat în martie 2003 de la <http://www.isesd.cv.ic.ac.uk/ESD/frameset.htm>
- Athanasopoulos, G.A., Pelekis, P.C., Leonidou, E.A. (1998). "Effects of surface topography and soil conditions on the seismic ground response - including liquefaction - in the Egion (Greece) 15/6/1995 earthquake". 11th European Conference on Earthquake Engineering, Balkema, Rotterdam.
- Bertero, V.V. (1997). "Earthquake Engineering" in Structural Engineering Slide Library, Golden W.G. (ed.), The University of Berkeley, California, USA.
- Chang, H-Y. and Kawakami, H. (2006). "Effects of ground motion parameters and cyclic degradation behaviour on collapse response of steel moment-resisting frames". Journal of Structural Engineering, Vol. 132, no. 10, pages 2553-1562.
- Chopra, A.K. (2004). "Estimating seismic demands for performance-based engineering of buildings". 13th World Conf. on Earthquake Engineering, Vancouver, B.C., Canada. Paper no. 5007.
- Cuesta, I., Aschheim, M.A., Fajfar, P., (2003). "Simplified R-Factor Relationships for Strong Ground Motions". Earthquake Spectra, Volume 19, No. 1, pages 25-45.
- De Martino, A., Faella, C. and Mazzolani, F.M. (1984). Simulation of Beam-to-Column Joint Behaviour under Cyclic Loads. *Costruzioni Metalliche* 6, 346-356.
- Della Corte, G., De Matteis, G. and Landolfo, R. (2000). Influence of Connection Modelling on Seismic Response of Moment Resisting Steel Frames. In: Mazzolani F.M., (ed.). *Moment resistant connections of steel buildings frames in seismic areas*, E. & F.N. Spon, London.
- Dubina, D. and Dinu, F. (2007). "High strength steel for seismic resistant building frames". Proc. of the 6th Int. Conf. on Steel and Aluminium Structures, 24-27 July 2007, Oxford, UK (in print).
- Eurocode 8: 1994. Design Provisions for Earthquake Resistance of Structures, part 1-1, 1-2, 1-3. 1994.
- Fajfar, P. (2000). "A nonlinear analysis method for performance-based seismic design". Earthquake Spectra, 16(3): 573-92.
- FEMA 356, (2000). "Prestandard and commentary for the seismic rehabilitation of buildings", Federal Emergency Management Agency, Washington (DC).
- FEMA 356. 2000. Prestandard and comentary for the seismic rehabilitation of buildings. ASCE. November, 2000.
- Fischinger, M., and Fajfar., P., (1994). "Seismic force reduction factors". in Earthquake Engineering. A. Rutenberg (editor), Balkema, pp.279-296.
- Gioncu, V., and Mazzolani, F.M. (2002). "Ductility of Seismic Resistant Steel Structures". Spon Press, London and New York.
- Jaspart, J.P. (2000). General Report: Session on Connections. *Journal of Constructional Steel Research* 55, 69-89.
- Lalkan, S.M. and Kunnath, S.K. (2006). "Adaptive modal combination procedure for nonlinear static analysis of building structure". Journal of Structural Engineering, Vol. 132, No. 11, pages 1721-1731.
- Lacave-Lachet, N., Bard, P.Y., Gariel, J.C., Irikura, K. (1998). "Straightforward methods to detect non-linear response of the soil. Application to the recordings of the Kobe earthquake (Japan, 1995)". 11th European Conference on Earthquake Engineering. Balkema, Rotterdam.
- Lungu, D., Aldea, A., Nedelcu, C., Cornea, T., (1998). "Use of the GIS technology for microzonation of the frequency content and effective peak values of soil response to earthquakes" 11th European Conference on Earthquake Engineering, Balkema, Rotterdam.
- Mazzolani, F.M. (1988). Mathematical model for semi-rigid joints under cyclic loads. In R. Bjorhovde et al. (eds) *Connections in Steel Structures: Behaviour, Strength and Design*, Elsevier Applied Science Publishers, London, 112-120.
- Möller, B. & Beer, M. 2004. *Fuzzy Randomness - Uncertainty in Civil Engineering and Computational Mechanics*. Berlin, Heidelberg: Springer.
- Möller, B., Beer, M., Graf, W. & Sickert, J.-U. 2001. Fuzzy Finite Element Method and its Application. In: W.A. Wall, K.-U. Bletzinger & K. Schweizerhof (eds) *Trends in Computational Structural Mechanics, Colloquium*: 529-538. Barcelona: CIMNE.
- Möller, B., Graf, W. & Beer, M. 2000. Fuzzy structural analysis using  $\alpha$ -level optimization. *Computational Mechanics* 26: 547-565.
- Möller, B., Graf, W. & Nguyen, S. H. 2004. Modeling the life-cycle of a structure using fuzzy processes. *Intern. Journal of Computer-Aided Civil and Infrastructure Engineering* 19: 157-169.
- Necevka-Cvetanovska, G. & Petrusavska, R. 1996. Non Linear Analysis of RC Structures using Computer Program INELA with Included Bank of Hysteretic Models. *Third European Conference on Structural Dynamics, EURO DYN '96* : 515-522. Florence. Italy.
- Necevka-Cvetanovska, G. & Gjorgjievska, E. 1998. "Application of the "capacity design" approach in design of earthquake resistant buildings in accordance with Eurocode 8", *Proceedings of XI ECEE*, Paris, France.
- Necevka - Cvetanovska, G. 1999. "A Method for Evaluation of the Seismic Resistance of R/C Building Structures", *ASPPRA' 99*, Taipei, Taiwan, feb.1-3, 1999, pp.426-435
- Necevka - Cvetanovska, G. & Petrusavska, R., 2000. "Methodology for Seismic Design of R/C Building Structures", *Proc. of the XII-th World Conference of Earthquake Engineering, (12WCEE)*, New Zealand.
- NEHRP 2000. Building Seismic Safety Council, BSSC (2001). "NEHRP Recommended Provisions for Seismic Regulations for New Buildings and Other Structures, Part 1 — Provisions and Part 2 — Commentary". Federal Emergency Management Agency, Washington D.C.
- Newmark, N., Hall, W., (1982). "Earthquake Spectra and Design", Earthquake Engineering Research Institute (EERI), Oakland, CA
- Nogueiro, P., Simões da Silva, L., Bento, R., Simões, R. 2005. Numerical Implementation and Calibration of a Hysteretic Model with Pinching for the Cyclic Response of Steel and

- Composite Joints. in *Fourth International Conference on Advanced in Steel Structures ICASS 05*. Shanghai, China.
- Nogueiro, P., Simões da Silva, L., Bento, R., Simões, R. 2005. Influence of Joint Slippage on the Seismic Response of Steel Frames. In *EuroSteel Conference on Steel and Composite Structures*, 8 to 10 June in Maastricht, The Netherlands.
- Nogueiro, P., Bento, R. and Simões da Silva, L., "Evaluation of the ductility demand in partial strength steel structures in seismic areas using static pushover analyses", in *Proceedings of the XI<sup>th</sup> International Conference Metal Structures*, Rzeszow, Poland, June 21-23 (2006).
- Nogueiro, P., Simões da Silva, L., Bento, R. and Simões, R., "Numerical implementation and calibration of a hysteretic model with pinching for the cyclic response of steel joints", *International Journal of Advanced Steel Construction*, - (in print 2006).
- EN 1998 (2005). "Eurocode 8: Design of structures for earthquake resistance. Part 1: General rules, seismic actions and rules for buildings". CEN - European Committee for Standardization.
- Priestley, M.J.N. 2000. Performance Based Seismic Design, *Bulletin of the New Zealand National Society for Earthquake Engineering*, v 33, n 3, Sep, 2000, p 325-346.
- Priestley, M.J.N. 2002. Direct Displacement-Based Design of Precast/Prestressed Concrete Buildings, *PCI Journal*, v 47, n 6, November/December, 2002, p 66-79.
- Sasani, M. and Bertero, V.V. (2000). "Importance of severe pulse-type ground motions in performance-based engineering: historical and critical review". Proc. 12th World Conference on Earthquake Engineering (12WCEE), New Zealand, paper 1302.
- SeismoStruct. (2004). "Computer program for static and dynamic nonlinear analysis of framed structures" [online]. Available from URL: <http://www.seismosoft.com>
- Shibata, A. & Sozen, M. 1976., Substitute Structure Method for Seismic Design in R/C, *Journal of Structural Division*, ASCE, January, 1976.
- Simeonov, B., et al. 1993. Static Analysis, Dynamic Analysis and Proportioning of the Structure of the Residential - Business Building B-2, Vardar Settlement, Skopje, Unit 4. *IZIIS Report 93-15*. Skopje. FY Republic of Macedonia.
- Simões, R., Simões da Silva, L. and Cruz, P. (2001). Cyclic behaviour of end-plate beam-to-column composite joints. *International Journal of Steel and Composite Structures* 1(3), 355-376.
- Stewart, J.P., Chiou, S-J., Bray, J.D., Graves, R.W., Someville, P.G., Abrahamson, N.A. (2001). "Ground Motion Evaluation Procedures for Performance-Based Design". PEER Report 2001/09, Pacific Earthquake Engineering Research Center, College of Engineering, University of California, Berkeley.
- Stratan, A. (2003). "Multistorey dual steel structures located in seismic areas" (in Romanian). PhD Thesis. Politehnica University of Timisoara.
- Terzic, U. 2006., Direct Displacement-Based Design of Reinforced Concrete Frame Building Structures. *Master Thesis, IZIIS, University "Ss. Cyril and Methodius", Skopje, FY Republic of Macedonia*.
- UBC (1997). Uniform Building Code Vol.2, International Conference of Building Officials, Whittier, CA.
- Vidic, T., Fajfar, P., and Fischinger, M., 1994. Consistent inelastic design spectra: strength and displacement, *Earthquake Eng. Struct. Dyn.* 23, 507-521.
- Whittaker, A., (n.d.) "Earthquake Engineering and Structural Dynamics II". accessed in March 2003 at: <http://overlord.eng.buffalo.edu/ClassHomePages/cie619/index.htm>
- Wilson & Habibullah. 1998. SAP 2000 - Three Dimensional Static and Dynamic Finite Element Analysis and Design of Structures, CSI, Berkeley University, California, 1998.
- XTRACT.Cross-sectional and Structural Analysis of Components, Imbsen Software Systems, [www.imbsen.com](http://www.imbsen.com).